بسم الله الرحمن الرحيم

Palestine Polytechnic University
Deanship of Graduate Studies and Scientific Research
Master of Civil Engineering- Earthquake Engineering

Response Modification Factor in Intermediate Moment Resisting Frame Building

Name of student

Hadeel Ali Abuznaid

Supervisor

Dr.Haitham Ayyad

Thesis submitted in partial fulfillment of the requirements of the degree of Master of Science in civil engineering to the faculty of Graduate Studies at Palestine Polytechnic University

August, 2023

The undersigned hereby certify that they have read, examined and recommended to the Deanship of Graduate Studies and Scientific Research at Palestine Polytechnic University

Response Modification Factor in Intermediate Moment Resisting Frame Building

Hadeel Ali Abuznaid

In partial fulfillment of the requirements for the degree of Master in Renewable Energy & Sustainability.

Graduate Advisory Committee:

Prof./Dr. ……, (Supervisor), University (typed)

Signature: _____Date: _____

Prof./ Dr. ……, (Co-supervisor), University (typed)

Signature: _____Date: _____

Prof./Dr……, (Internal committee member), University (typed).

Signature: _____Date: _____

Prof./Dr. ……, (External committee member), University (typed).

Signature:———————— Date:————————

Thesis Approved by:

Name:

Dean of Graduate Studies & Scientific Research

Palestine Polytechnic University

Signature: _____Date: _____

DEDICATION

اهدي هذا البحث المتواضع...

- الى من أهدتني الحياة... منبع الحنان، ومنهل العطاء أمي الحبيبة
- الى من كان لي عونا وسندا ثابتا في الحياة... أبي الغالي
- الى أجمل من أضاف الى حياتي حياة، ورفيق دربي ... زوجي الغالي
- الى فلذة كبدي، ومهجة قلبي، وقرة عيني... ابنتي الحبيبة ألما.

ACKNOWLEDGEMENT

أتقدم بالشكر والتقدير وعظيم الامتنان لله أولاً وقبل كل شيء.. ثم الى منارة العلم جامعي الغالية جامعة بوليتكنيك فلسطين، بكل كوادرها الاكاديمية والادارية.

كما أتقدم بالشكر الجزيل لمشرفي على هذه الرسالة الدكتور هيثم عياد والذي لم يتوانى لحظة عن تقدم يد العون والمساعدة والنصح والارشاد لإنجاز هذا العمل ليخرج الى حيز الوجود بالشكل الذي هو عليه.

كما أتقدم بالشكر لرئيس دائرة الهندسة المدنية ومشرف برنامج ماجستير الهندسة المدنية الدكتور بلال المصري.

وأخص بالذكر د. إبراهيم الهشلمون الذي قام مشكورا بالاطلاع على الرسالة وتنقيحها, فكان له الأثر الكبير في ترتيب وتنسيق الجمل المختلفة فيها.

وأتقدم بالشكر لكافة اساتذتي في برنامج الماجستير وزملائي وزميلاتي. وكل من ساهم في اتمام هذا العمل المتواضع.

ABSTRACT

The response modification factor (R) is considered as one of the most important parameters that affect the seismic design of new buildings all around the world. Any improvement in the reliability of modern earthquake-resistant buildings around the world must involve an exhaustive examination of the building response characteristics that have the greatest influence on the values assigned to the factor. The primary goal of this analytical and parametric research is to examine the response modification factor (R) and study the seismic behavior of the buildings in Concrete Moment Resisting Frame System (CMRFS) structures constructed. The research focuses on an Intermediate Moment Resisting Frame System (IMRFS), with 4 and 3 bays in longitudinal and transverse directions for 1,2,3 and 4 stories, each one consists of (18x24) m^2 two-way solid slab with 6m center to center span between columns. Nonlinear behavior is applied for beams and columns due to gravity and earthquake loadings. A nonlinear static pushover analysis (fiber hinges) is performed and compared with the available published experimental data. The capacity curve of the structure using the displacement control approach is used to evaluate the response modification factor (R) and is compared with the ASCE code values. A parametric study is carried out to investigate the realistic value of the response modification factor. In this parametric study, the effect of number of stories, size of column section dimensions, member reinforcement and performance point are investigated. Results of this research show that the number of stories and the difference of columns cross sections as well as the maximum lateral displacement that is imposed on the structure during the pushover analysis have a substantial impact on the R-factor value. This research evaluates the pattern and explains the relationship of change in R-factor with an increase in the number of stories and decrease the cross-sectional areas and the redundancy factor and suggesting the real value of (R) for a different number of stories that are exposed to the same conditions and linking it to the values of the Performance Point (PP) and the Performance level of structures against earthquakes.

Table of Contents

LIST OF FIGURES

LIST OF TABLES

CHAPTER 1:INTRODUCTION

1.1 Background

Given the significant impact and destruction caused by natural disasters such as earthquakes on various buildings and facilities, the world has given more attention to studying and understanding such phenomena and how to predict, resist and reduce the resulting damages.

While loads are usually presented in terms of force, earthquake load is presented in terms of ground motion. Moreover, while static loads are constant, earthquake loads are dynamic and can change rapidly in a very short period of time. Moreover, unlike other loads that predominantly act vertically, an earthquake load can exert forces simultaneously in both horizontal and vertical directions (Hu YX et.al 1996).

The Moment Resisting Frames systems (MRFS) are commonly used as a component of Seismic Force Resisting System (SFRS) due to their high energy dissipation and superior deformation. These frames are composed of columns and beams that are rigidly connected to each other in a manner that makes them resist both lateral and gravity loads (Han SW, Jee NY 2005). MRFS are classified according to the American Concrete Institute into three types: Ordinary Moment Resisting Concrete Frame (OMRCF); Intermediate Moment Resisting Concrete Frame (IMRCF); and Special Moment Resisting Concrete Frame (SMRCF) (ACI 318 2002).

The design and detailed reinforcement specifications for each type of moment frame and seismic risk level are outlined in the ASCE 2016 guidelines. The choice of moment frame type is dependent on the seismic design category or risk, determined by parameters such as the design spectrum response acceleration at short period or 1- sec period S_{DS}; S_{D1}, respectively. In alignment with the seismic risk, the appropriate moment frame type should be selected. In regions with low to moderate seismic activity, the commonly used moment resisting frames are OMRCF and IMRCF. However, the design and reinforcement criteria for these frames are less strict compared to those for SMRCF. For IMRCF and SMRCF frames, specific detailing is important to ensure ductile behavior, in contrast with the requirements for OMRCF.

1.2 Problem Statement

The strength of the previously mentioned MRCF types is influenced by numerous design factors, such as the response modification factor (R), which is still under study and the attention of researchers until now. This is because the utilization of response modification factor exceeding one will almost inevitably lead to compliance with building codes resulting in seismic design yielding. Various factors, including ground motion characteristics and the arrangement of stiffness and mass distributions horizontally and vertically within the building, will impact the extent and distribution of yielding or inelastic response (Whittaker A et al, 1999). As a result, the design and analysis intricacies of the building are significantly influenced by these values.

1.3 Research Objectives and Methods

The objective of this research is to evaluate the actual behavior of an Intermediate Moment Resisting Concrete Frame (IMRCF) when subjected to seismic loads (earthquakes) while varying the response modification factor values. This objective is achieved by utilizing numerical methods to verify the proposed nonlinear analytical approach through a finite element investigation conducted using the SAP2000 software. The software facilitates the parameterization of various seismic frame element types. The finite element modeling implemented in this study involves a nonlinear analysis of fiber hinges within the intermediate moment resisting frame components. This analysis aims to determine the effect of the ASCE code's response modification factor on the ultimate behavior of the frame building. This is achieved by applying different values of this factor within the range of 1 to 7 for varying numbers of stories (Ground, first, and second floors) and different cross-sectional areas of column elements. The goal is to determine the most appropriate value for each case.

1.4 Scope of the Research

The scope of this research is limited to parametric and analytical modeling, employing computer-based methods alongside numerical techniques. The primary focus of the study lies in investigating the impact of the response modification factor's value on the actual

behavior of the Intermediate Moment Resisting Concrete Frame System (IMRCF) elements when subjected to seismic loading (earthquakes). The research also delves into determining the actual value of the response modification factor (R) across various conditions, including the number of stories and redundancy factor.

The research encompasses the design and modeling of frame elements, engineered to withstand earthquake-induced strength and displacement, thus averting potential failure. Additionally, it explores the influence of certain code parameters on this frame strength and the interconnected factors that these parameters are influenced by.

1.5 Research Significance and Impacts

This research presents a parametric and analytical study examining the actual behavior of concrete seismic frame subjected to an earthquake. This includes examining frame elements behavior in a regular multi-story building system which is braced by a two-way concrete solid slab. The investigation highlights the influence of this structural setup, alongside the code's response modification factor, on the strength of the frame elements. Additionally, the research provides insights into considerations for stability in the design of concrete seismic frame components.

The impact of this research may lead to the development of a more comprehensive and rational approach for designing and analyzing seismic concrete frames. Such an approach could result in designs that are not only safer but also more cost-effective. The outcomes of this study might contribute to modifying certain code parameters or proposing new equations and values tailored to different building types, ultimately affecting structural strength and maximum lateral displacement. Furthermore, these findings could aid in identifying structures suitable for retrofitting in cases where existing frame elements were originally under designed.

CHAPTER 2:BACKGROUND AND LITERATURE REVIEW

2.1 Background

2.1.1 Response Modification Code Factor (R) Background

Structures are typically initially designed using equivalent static forces as defined by building codes. These static forces are inherently based on fundamental elastic vibration modes. Since achieving complete safety and robustness during construction is not feasible, current structural design codes incorporate the possibility of a credible earthquake occurring (ATC3-06, 1978). However, utilizing an inelastic energy dissipation system allows for the analysis of various structural and nonstructural damages, enabling the attainment of a high level of safety in structural design in an economical manner. The majority of seismic codes permit a reduction in design loads by acknowledging that structures possess a significant amount of reserve strength and energy dissipation capability (ductility Rμ). The parameter R encapsulates these characteristics within the structural framework (Kim et al., 2005). When designing for lateral strength, it's common for the actual lateral strength to be lower than what seismic standards stipulate as necessary for structures to remain within the elastic range.

One important aspect in the design of seismic structures is the response modification factor (R). This factor may be used to implement equivalent statistical analysis, which is widely used to estimate the seismic response of structures. R specifically denotes a structure's capacity to release energy through inelastic behavior, as shown by current building rules. Several researchers like (Wu et al., 1989; Hanson et al., 1993) investigated the impact of R on the ability of a structure to dissipate energy. When applied to concentrically braced frames, (M Bosc et al.'s, 2013) prediction of height-wise damage during eccentrically braced frame (EBFs) collapse. (Galasso et al., 2014) claim that code provisions are not conservative and that they serve as a foundation for future editions of building seismic design codes to be calibrated more accurately. From capacity curves produced using various Adaptive pushover analysis (APA) and conventional pushover analysis (CPA) techniques, (Izadinia et al., 2012) derived a derivation of parameters like, and R. R was assessed for concrete bridges in Europe by (Kappos et al., 2013). The comparison of equations for the design base shear for an elastic response (V_e) (Eq.2) and an equation for an inelastic response (Eq.1) demonstrates the effect of R on building seismic design.

$$V = \frac{2.5Aa}{R} W \quad (1)$$

$$V_e = S_{e,5}W \quad (2)$$

Where ($S_{e,5}$) is the elastic 5-percent damped pseudo acceleration response spectral ordinate and (A_a) is the effective peak acceleration of the design ground motion. The quantity ($2.5A_a$) in Eq. (1) is equal to the elastic spectral ordinate in Eq (2). If R=1.0 in Eq. (1), then equations (1) and (2) are the same. By dividing the base shear force elastic response by R, a number that typically ranges between 4.0 and 8.0 (ATC, 1995), it is possible to get the design base shear (for inelastic response).

R is the ratio of forces that would rise in the structure if the behavior were totally elastic compared to the prescribed design forces at the level of significant yield (ATC, 1978). R lowers the design value of the base shear for the design earthquake, ensuring that the structure may enter the inelastic range if the design earthquake or a larger event happens (see Figure 2-1). To generate the design spectrum for a specific structure type, each point on the normalized elastic response spectrum is divided by R (ATC, 1995).

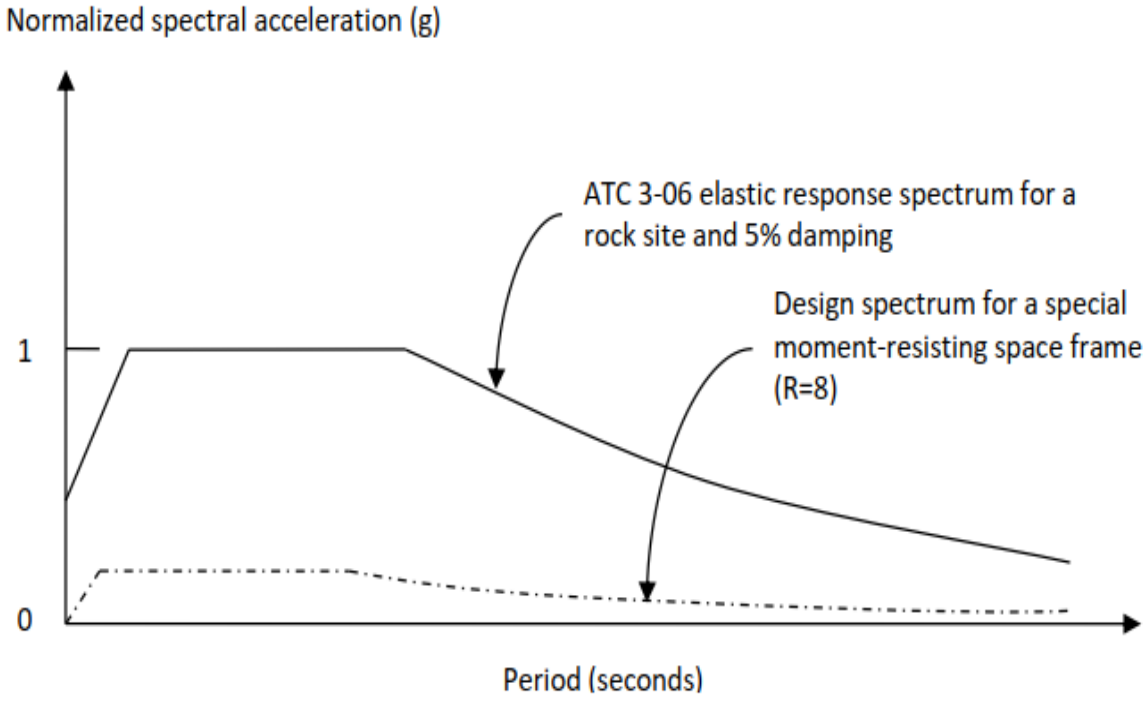

Figure 2.1: Use of R Factors to Reduce Elastic Spectral Demands to The Design Force Level (ATC-19).

R is the most important component to consider in the seismic design process, however it is still debatable. No other parameter in the design base shear equation influences the design action in seismic framing systems as much as the value assigned to R, Ω and Rμ factors for major seismic framing systems differ according to seismic zone due to differences in gravity load to seismic load proportions. (Abdi H et al, 2018).

Since the initial formulation for R was proposed, extensive study has been done (ATC, 1982B; Freeman, 1990; ATC, 1995). A newly proposed formulation for R that expresses R as the products of three components is supported by recent investigations, including those in the companion project ATC-34 Eq (3):

$$R = R_S R_\mu R_R \tag{3}$$

Where Rs is the period-dependent strength factor, Rμ is the period-dependent ductility factor and R_R is the redundancy factor.

Figure 2-2 demonstrates how the pushover curve is used to evaluate over-strength and ductility factors, which are important component elements in the R formulation. The following is a description of the parameters in this figure: Max base shear force (V_μ), max displacement (Δ_{max}), design base shear force (V_d), displacement resulting from the design base shear force (Δ_w), base shear force versus roof displacement relationship at yield point (V_y), and roof displacement relationship at yield point (Δ_y) (Abdi H et.al., 2019).

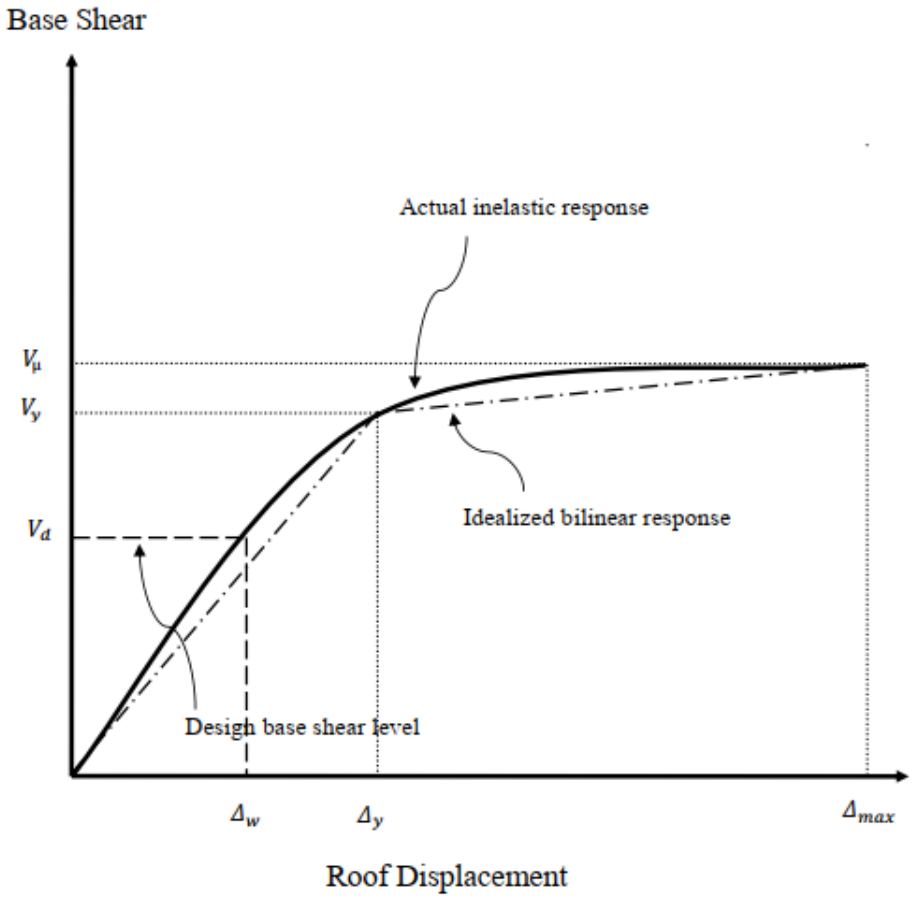

Figure 2.2: Idealization of Inelastic Response of Structure.

2.1.2 Seismic Force Resisting System Background

There is a strong correlation between the earthquake-resistant system and building strength, as evident in the lateral force reduction factor that distinctly links the building's design base shear to the earthquake-resistant system. This link stems from the precise detailing requirements intrinsic to each system's design, with ductility and seismic resistance being interconnected (Eberhard MO, 1995). The Seismic Force Resisting System (SFRS) of a structure bears the responsibility of withstanding the lateral forces generated by seismic events.

These inertial forces must be transferred from the horizontal parts diaphragm to the vertical (SFRS) parts during a seismic event. Depending on the kind of diaphragm being utilized, these forces are transferred directly in a certain way. In any case, the diaphragm and the (SFRS) both transfer and resist forces in different ways, which are described by basic design approximations. These approximations describe this behavior by segmenting the

diaphragm into collectors and chords. The chords must be able to withstand both moment and shear demands. A simple beam idealization can be showing the distribution of these forces, see Figure 2-3(a) (Moehle 2016). In order for such behavior to be true, “then equilibrium requires that the diaphragm shear be distributed uniformly along the depth of the diaphragm” (Moehle 2016). These uniform shear/axial forces must be transferred to the (SFRS) by the collector elements. Figure 2-3(c) illustrates how additional reinforcing is added to the slab of a concrete construction to withstand these stresses.

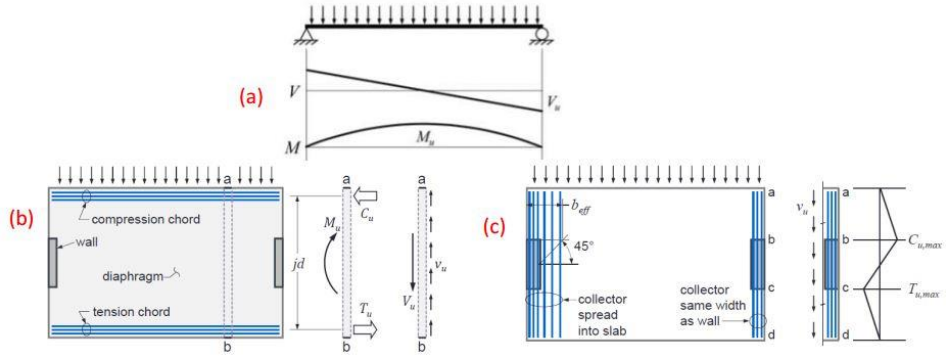

Figure 2.3: Diaphragm Force Distribution (Moehle 2016)

2.1.3 Reinforced Concrete Structure Elements Background

The reinforced concrete structures consisting of a horizontal diaphragm (HD) is defined as the structural member that conveys acting forces in the member's plan to the vertical elements of the seismic-force-resisting system, such as a floor or roof slab (ACI 2008). The diaphragm design is usually limited to the elastic range (Vassallo D et.al. 2013, Sullivan K 2018, Moroder D 2016, Fast P et al 2017). According to the relative stiffness between the horizontal diaphragm and the vertical parts, the horizontal diaphragm behavior is characterized as either a rigid diaphragm Figure 2-4(a) or a flexible diaphragm Figure 2-4(b). Since a rigid diaphragm takes into account torsion and distributes horizontal forces over the vertical parts by virtue of its rigidity, each of these models places different demands on the vertical elements than a flexible diaphragm, which does so by virtue of the idea of tributary area.

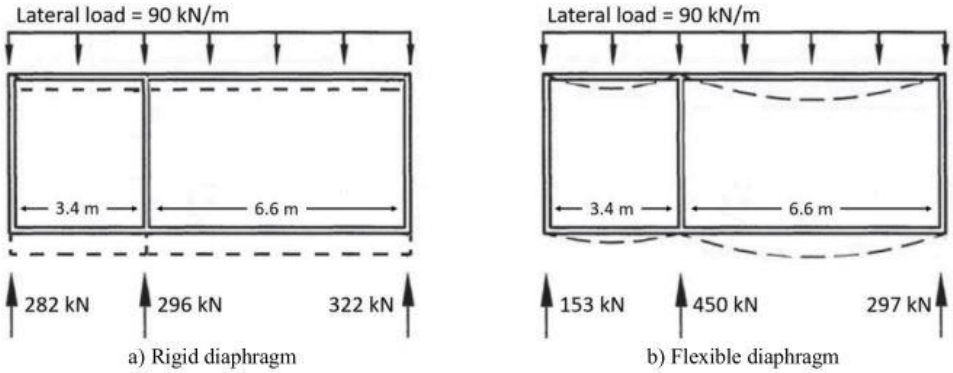

Figure 2.4: Horizontal Diaphragm Behavior. a) Rigid Diaphragm, b) Flexible Diaphragm.

It is assumed that the forces entering the vertical elements are collected in beams that are parallel to these elements. Typically, a line of collector beams is offered, extending the entire depth of the diaphragm. In this collector beams line, the forces increase linearly from zero at the diaphragm edge to the point where the vertical elements take the forces. This occurs at the positions of the columns for moment frames, at a single point or a number of sites where the braces meet for braced frames, and in a distributed manner for shear walls (see Figure 2-5).

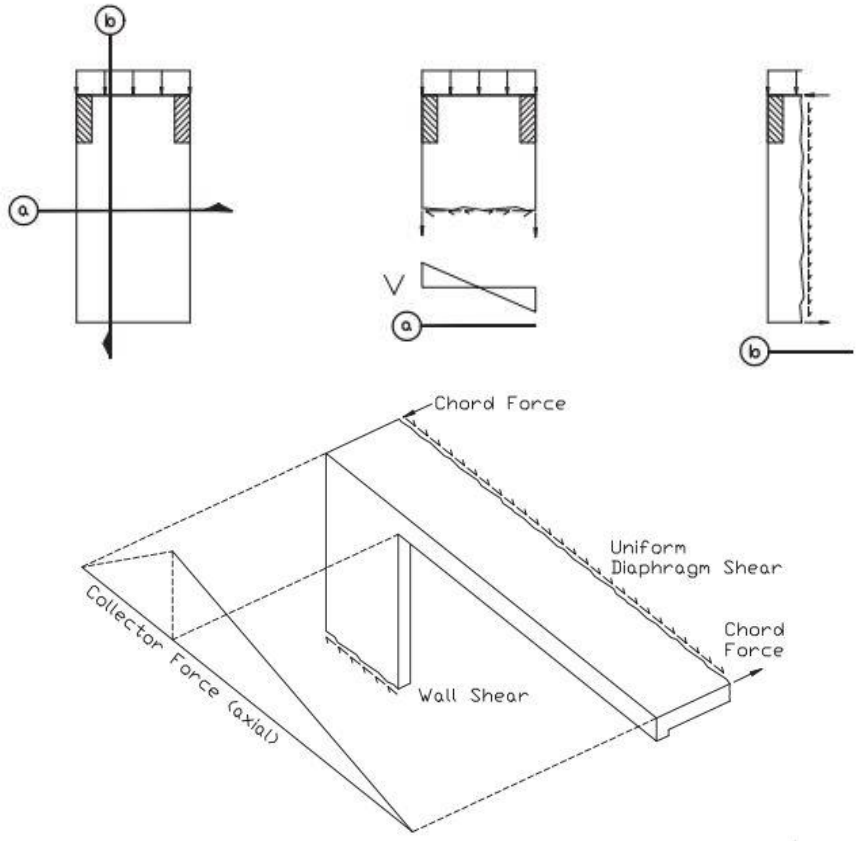

Figure 2.5: Linear Collector Diaphragm.

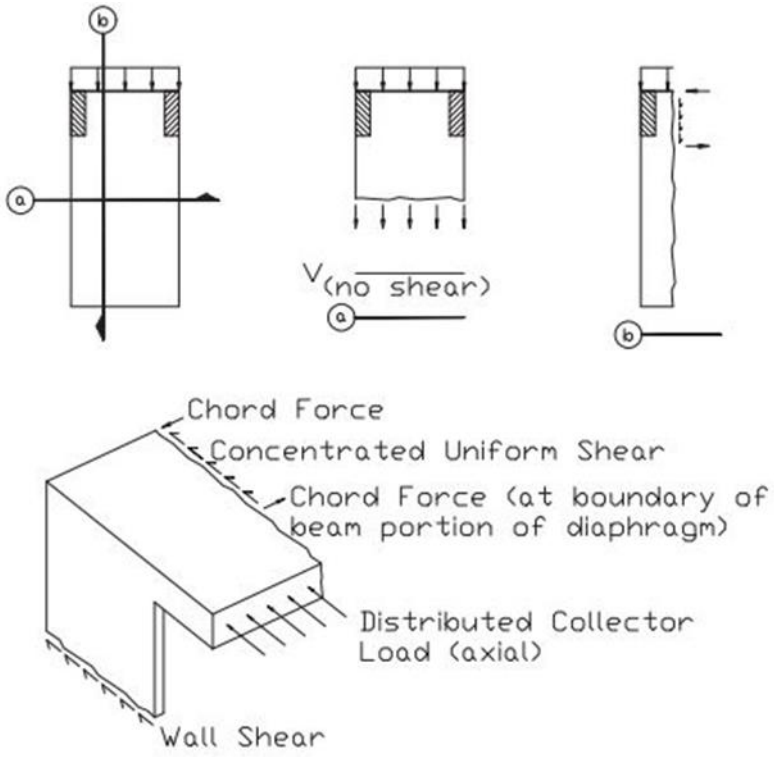

Figure 2.6: Distributed Collector Diaphragm.

A mechanism is also needed to transfer the force to the diaphragm's shearing regions. (See Figure 2-6) for an extreme example where the full width of the diaphragm could be thought of as acting as a dispersed collector and only a small piece of the diaphragm could be thought of acting as the beam (with the smaller depth leading to larger chord forces) (Rafael Sabelli PE et al 2009).

2.2 Literature Review

In the seismic design of new buildings, the response modification factor is critical. The thorough assessment of the building response characteristics that have the greatest impact on the values assigned to the response modification factor is an essential requirement for any development in the dependability of present-day earthquake-resistant buildings. In order to do this, the research proposes a draft formulation that models the response modification factor as the sum of variables relating to reserve strength, ductility, and redundancy. Relevant information from numerous experimental and analytical research on reserve strength and ductility is also provided (Whittaker A et al 1999). In another

research, ductility and response modification factor of Buckling Restrained Braced frames were evaluated. To do so, buildings with various stories and different bracing configuration including diagonal, split *X*, chevron (*V* and Inverted *V*) bracings were considered. Static pushover analysis, nonlinear incremental dynamic analysis and linear dynamic analysis have been performed using Open-Sees software. The effects of some parameters influencing response modification factor, including the height of the building and the type of bracing system, were investigated. In this article seismic response modification factor for each of bracing systems has been determined separately and tentative values of 8.35 and 12 has been suggested for ultimate limit state and allowable stress design methods (Asgarian B and Shokrgozar HR 2009). (Mahmoudi M and Abdi MG 2012) Evaluated overstrength, ductility, and response modification variables in triangular-plate added damping and stiffness (TADAS) devices for unique moment resisting frames. Actually, multi-story structures were taken into account while the study was being conducted. Static pushover analysis, nonlinear incremental dynamic analysis, and linear dynamic analysis were also performed using OpenSees Software. The seismic response modification factor for special moment resisting frames (SMRFs) with and without TADAS devices (T-SMRFs) has been independently determined in this study. The findings demonstrated that T-SMRFs had larger response modification factors than SMRFs. The number of stories in buildings was also found to have a higher impact on the response modification elements.

The application of pushover analysis has evolved recently, and several advanced pushover methods have been put forward to take into account the realistic behaviors of structures, such as the impact of higher modes or the impact of modifications in the structural modal characteristics during the analysis as a result of member yielding. The effect of near- and far-field data was thus taken into account using the adaptive pushover technique. The two views of strength and ductility can be used to separate the factors impacting the R factor in general. With and without frictional dampers in various locations and positions, structural analysis has been done using the finite element approach and accounting for the nonlinear manner of the members in an extended fiber section method. The findings highlight how, on average, the R factor has grown by 52.45% under various circumstances. Therefore, a new equation (Rd) is proposed for the R factor of structures along with a friction damper (slip force, number of stories, and bay of equipped with damper), based on the findings of numerous cases and the application of dampers with different slip loads and the variable number of dampers in each story (Sadeghi A et.al. 2021). In a predictive seismic risk

framework, (Badal and Sinha, 2019) provided the quantification of response reduction factor values for the reinforced concrete frame buildings. (Ali Akbari and Shariatmadar 2019) In their study and definition of the response modification factor of the moment-resisting frame with steel vertical slit panel (SSP-MRF).

In comparison to the values recommended in the India Design codes, (Mondal et al. 2013) estimated the actual value of the response-modification factor for the real reinforced concrete (RC) moment frame structure. They found that the values of the behavioral coefficient presented in the standard Indian regulations are higher than the actual response-modification factor. The R-factor of RC frames with various geometric configurations, including the number of stories, bays, bay width, and story height, was estimated by (Abou-elfath and Elhout 2018). (Izadinia et al 2012) used the capacity curve generated by applying conventional pushover analysis and adaptive pushover analysis to improve the definition of the coefficients, such as over-strength (Ω), ductility (R), and response-modification factor (R). Directivity effect and fling step effect are the two main impacts that are associated with near-field earthquakes. Recently, a study was carried out to determine the R factor of a moment-resisting RC frame created using a limit state design methodology by (Chen et al. 2017), (Zeynalian et al 2018), and (Asghari and Zamagh 2017). In order to lower the response-modification factor and the over-strength factor for all pushover methods, (Siahpolo et al 2016) estimated the response-modification factor of the steel moment frame using an adaptive pushover approach. (Abdi H et al 2019) made a review article on overstrength, ductility, and R tries to compile pertinent data from various experimental and analytical research.

(Fanaie and Dizaj 2012) calculated ductility and response modification factors for frames braced with a different type of buckling restrained braces, the results shown that the type of BRBF (Buckling Restrained Braced Frame) had greater overstrength, ductility, and response modification factors than conventional types, and it exhibits better seismic performance while also removing some of the drawbacks of conventional BRBF, such as low post-yield stiffness.

The procedure for determining a bridge's real response modification factors (q or R) is presented in (Kappos AJ et al 2013) research, and it is then applied to seven concrete bridges that are typical of the stock found in southern Europe. Pushover curves created for

the bridge in (at least) its longitudinal and transverse orientations are typically used to analytically estimate the R-factor, it is discovered that the force reduction factors that are available in all situations are higher than those that are utilized for designs that adhere to either Eurocode 8 or AASHTO criteria. (Abdi H et al 2018) study looked into how the response modification factor would change if viscous damper devices were used in reinforced concrete structures.

To determine the values of the response modification factors, reinforced concrete structures with various story counts were taken into consideration. Using finite element software, a nonlinear statistical analysis was carried out and suggested an equation based on the values of the damping coefficients to compute the response modification factors for reinforced concrete structures equipped with viscous damper devices in light of the analytical results across various scenarios. The inelastic seismic response of an RC building with a control system was also studied by (Hejazi et al 2011). Their nonlinear analysis of a structure equipped with viscous dampers revealed that these devices efficiently lessen structural motion and building damage during powerful earthquakes. A control system that has been optimized by (Hejazi et al 2013) for an earthquake energy dissipation system significantly lowers the seismic response of structures, increasing building safety during earthquake excitation. On the basis of these mechanisms and the building's pushover analysis, (Daza 2010) examined the connection between response modification factors and the minimal building strength and highlighted the connection between the R factor and the building's vital strength.

CHAPTER 3: STUDY DESCRIPTION

3.1 Prototype Structure Description

The proposed prototype structure in this research is firstly a one-story educational building with four bays in the x-direction and three in the other direction. A three-meter story height was designed as an Intermediate Moment Resisting Reinforced Concrete Frame (IMRCF), containing twenty (50x50) cm columns, nine (50x45) cm primary drop beams, and a two-way 250 mm solid slab. Then, a number of stories were added with the same previous specifications. The design loads and parameters were adopted from (ASCE 2016). Figures (3-1) and (3-2) shows the dimensions and layout of the one-story and multi-story structure building respectively, which were adopted in this research. Some of these dimensions will be changed later in the research to study their impact on the ultimate behavior of IMRCF, such as the dimension of columns.

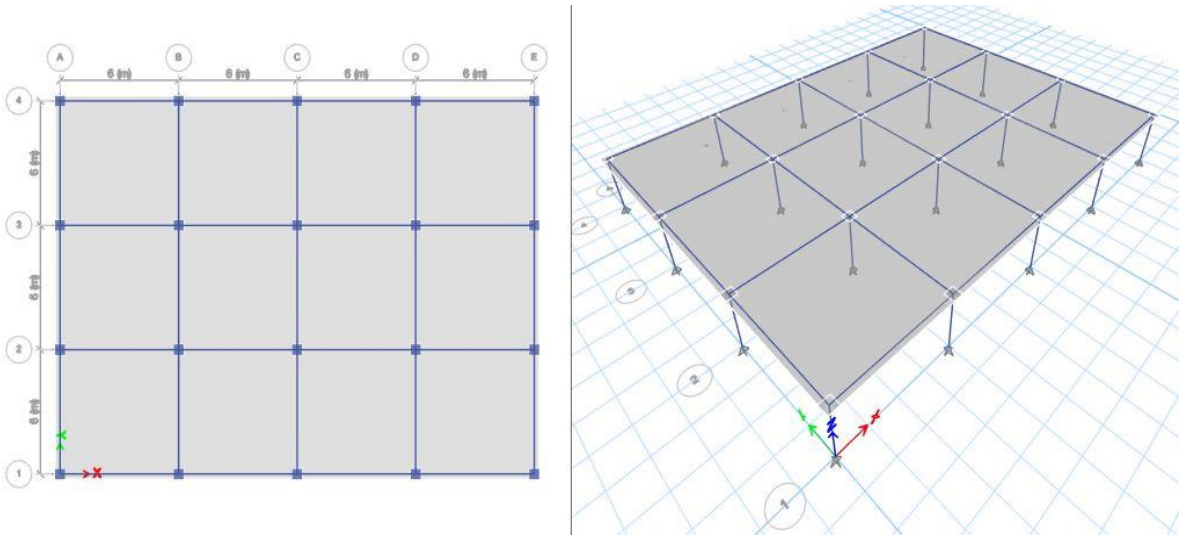

Figure 3.1: The Dimension and The Layout of The One-Story Structure Building.

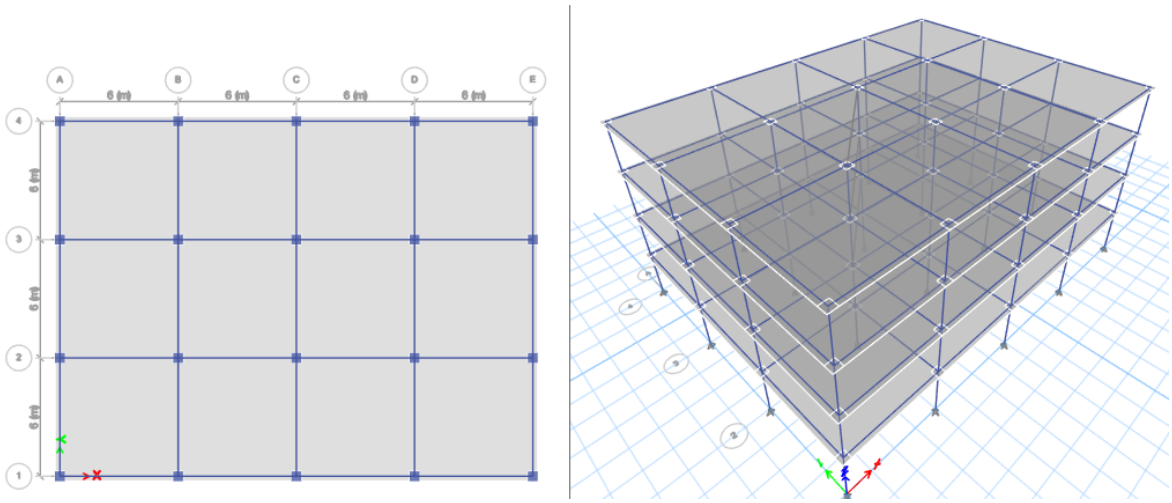

Figure 3.2: The Dimension and The Layout of The Multi-Story Structure Building.

The specified compressive strength (fc`) of concrete was assumed to be 24 MPa. The longitudinal reinforcement and the reinforcement for stirrups and hoops were assumed to have a yield strength (f_y) of 420 MPa. Design loads for the building were used (5kN/m^2 for dead load, excluding the self-weight, and 3kN/m^2 for live load). The section of all columns and beams in the model frame were assumed to be 500 mm x 500 mm and 500 mm x 450 mm, respectively.

The supposed structure is located in a high seismic design category region. Geographically, it is located near to Jericho City, West-Bank, Palestine. The design criterion for determining design forces is shown below.

Table 3.1: Design Conditions and Site Class Specific Factors, per ASCE 7-16

Design Code	ASCE 7-16
S_s	0.75
S_1	0.375
Soil Site Class	A Hard Rock
F_a	0.8
F_v	0.8
$S_{ms} = F_a * S_s$	0.6
$S_{m1} = F_v * S_1$	0.3
$S_{Ds} = 2/3\ S_{ms}$	0.4

$S_{D1} = 2/3\ S_{m1}$	0.2
Intermediate Reinforced Concrete Moment Frames	R =5, Ω =3, C_d = 4.5
Seismic Design Category	D
Occupancy Category	III (I_e = 1.25)
Number of Stories	1

3.2 Prototype Structure Design Forces

The design forces for the prototype structure are determined using the Equivalent Lateral Force (ELF) Method. To aid in determining the prototype structure's weight, a gravity load design was completed. Table 3-2 displays the required area of steel according to ACI 18.4 design code (As req. mm^2), the provided reinforcement, the values of which have been taken from ETABS 18.1.1, and the nominal and probable moment (ΦMn, Mn (kN.m)) respectively. The value of shear reinforcement is 2Φ10/100 mm on center with one located at 50 mm from the face of support for the collectors. Concerning the columns, Figure 3-3 displays the columns reinforcement and transvers design details.

Table 3.2: Design of The Reinforced Concrete Frames, per ACI-318 (18.4)

The edge frames (1, 4 and in the other direction A, E) Reinforcement For R=5					
Location		As required (mm^2)	Reinforcement	ΦMn (kN.m)	Mn (kN.m)
End Span	Left	663	6Φ14	134.8	149.8
		640 use Min 675	6Φ12	100.3	111.4
	Right	904	6Φ14	134.8	149.8
		566 use Min 675	6Φ12	100.3	111.4
Mid Span	Left	799	6Φ14	134.8	149.8
		500 use Min 675	6Φ12	100.3	111.4
	Right	741	6Φ14	134.8	149.8
		473 use Min 675	6Φ12	100.3	111.4

The mid frames (2, 3 and in the other direction B, C, D) reinforcement For R=5					
Location		As required (mm^2)	Reinforcement	ΦMn (kN.m)	Mn (kN.m)
End Span	Left	803	7Φ16	200	222.2
		640 use Min 675	6Φ12	100.3	111.4
	Right	1356	7Φ16	200	222.2
		640 use Min 675	6Φ12	100.3	111.4
Mid Span	Left	1187	7Φ16	200	222.2
		633 use Min 675	6Φ12	100.3	111.4
	Right	1084	7Φ16	200	222.2
		591 use Min 675	6Φ12	100.3	111.4

ΦMn(+ve) > ΦMn(-ve)/3 OK.

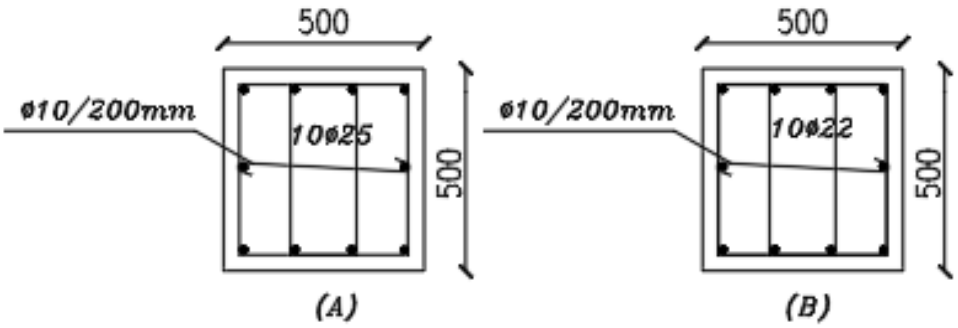

Figure 3.3: Columns Reinforcement and Transvers Design Details (A. For Columns on Axes A and E) (B. For the Other Columns).

CHAPTER 4: VEREFICATION AND NUMIRICAL APPLICATIONS

4.1 Chapter Layout

This chapter presents the implementation of the proposed nonlinear static analysis method. Various reinforced concrete structures which have been experimentally tested previously are employed in this study to validate the results of the computer simulation. The main focus of this chapter is to verify the accuracy of the analysis method that is conducted by the computer program of SAP2000. Important considerations for nonlinear modeling are also discussed employing the experimental results, with the aim of providing a general modeling application guide.

The structures considered for the validation purposes include two experimental reinforced concrete beams and a frame.

The first structure is a single span beam tested by (Bresler and Scordelis, 1963). The beam is simply supported, subjected to a concentrated point load at mid-span which presents a shear span to the effective depth ratio of about 7. A brittle failure resulting from a flexure-compression action was the type of failure experimentally observed for the beam.

The second structure is a simply supported reinforced concrete beam, continuous over two spans. The beam was experimentally tested by (Duddeck et al., 1976) and reported by (Mueller, 1977). The experimental data available to the author are those specified in ref. (Mueller, 1977). In contrast with the first analyzed beam, this beam exhibits a large nonlinear response before collapse occurs. Extensive cracking and yielding of concrete are observed, as well as a large nonlinear steel behavior. In fact, Dudeck's beam is a good and simple example on which to perform numerical tests concerned with the nonlinear solution procedure.

Finally, the third structure is a one-story frame of reinforced concrete which was experimentally tested by (Xiao et al., 2006). The details of those structures are mentioned in detail in the following sections.

4.2 Analysis Parameters and Material Properties

Any software program that does a nonlinear analysis like SAP2000 24 typically requires the user to choose a number of parameters or models. These could include nonlinear analysis choices like large displacements or hinge unloading techniques, as well as material models like the concrete tensile or compressive response models. The

displacement method for analysis is the most widely used approach in nonlinear material analysis problems (Bathe K. 1996). This method uses a step-by-step solution process because it is based on flow theory.

The application of the step-by-step method results in probable error at the end of each step, and this error will compound in the ones that follow. Even though the step-by-step procedure's efficiency has been improved with numerous innovative ways (Simo JC, Govindjee S., 1991, Simo JC, Taylor RL., 1985), these issues still cannot be avoided. Furthermore, to capture the change from elastic to plastic behavior, substantial mesh refinement is frequently needed. As a result, a number of scholars (such as (Hu W, Thomson PF., 1996, Kaljevic I et.al., 1996, Spacone E et.al. 1996)) have focused on using the force technique to examine structural issues involving nonlinear materials. Instead of the nodal displacements as in the displacement technique, the primary unknowns in this method are the internal element forces. This frequently offers a far more effective depiction for elastoplastic issues. The elastic perfectly plastic model of stress strain diagrams was adopted in the numerical application according to the values of slope hardening were obtained from the experimental studies as shown in Figure 4-1.

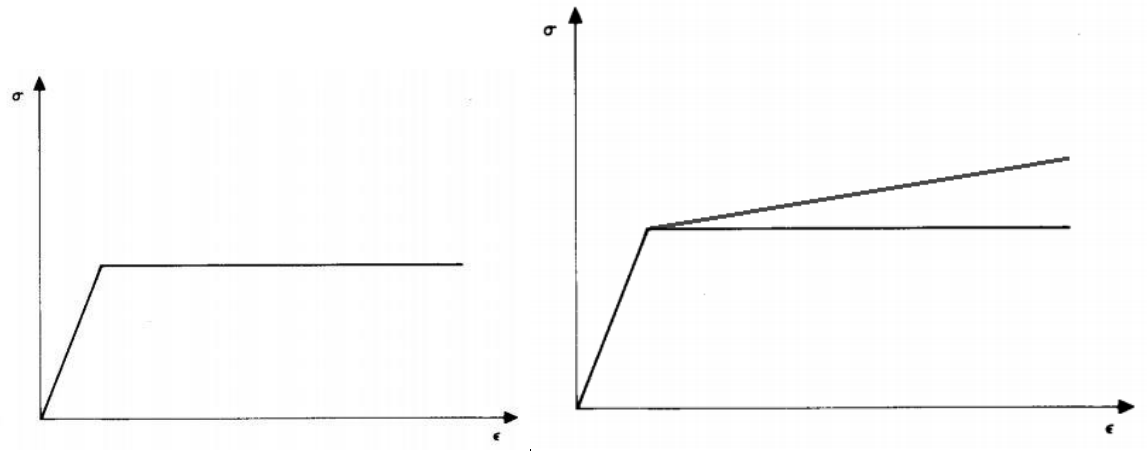

Figure 4.1 a. Elastic-Perfectly Plastic Stress-Strain Curve. b. Elasto-Plastic with Linear Hardening Stress-Strain Curve.

4.2.1 Single Span Beam

For the first single span reinforced concrete beam with (56.134x30.734) cm^2 cross section area that had a (2#4 and 6#9) longitudinal reinforcement for compression and tension regions respectively. The elevation, cross section and reinforcement details of the beam are illustrated in Figure 4-2, and the material properties of the single span beam are specified in Table 4-2. It presents identical steel properties and slightly different properties for concrete. The material parameters for concrete are given in (B. BRESLER and A. C. SCORDELIS, 1963).

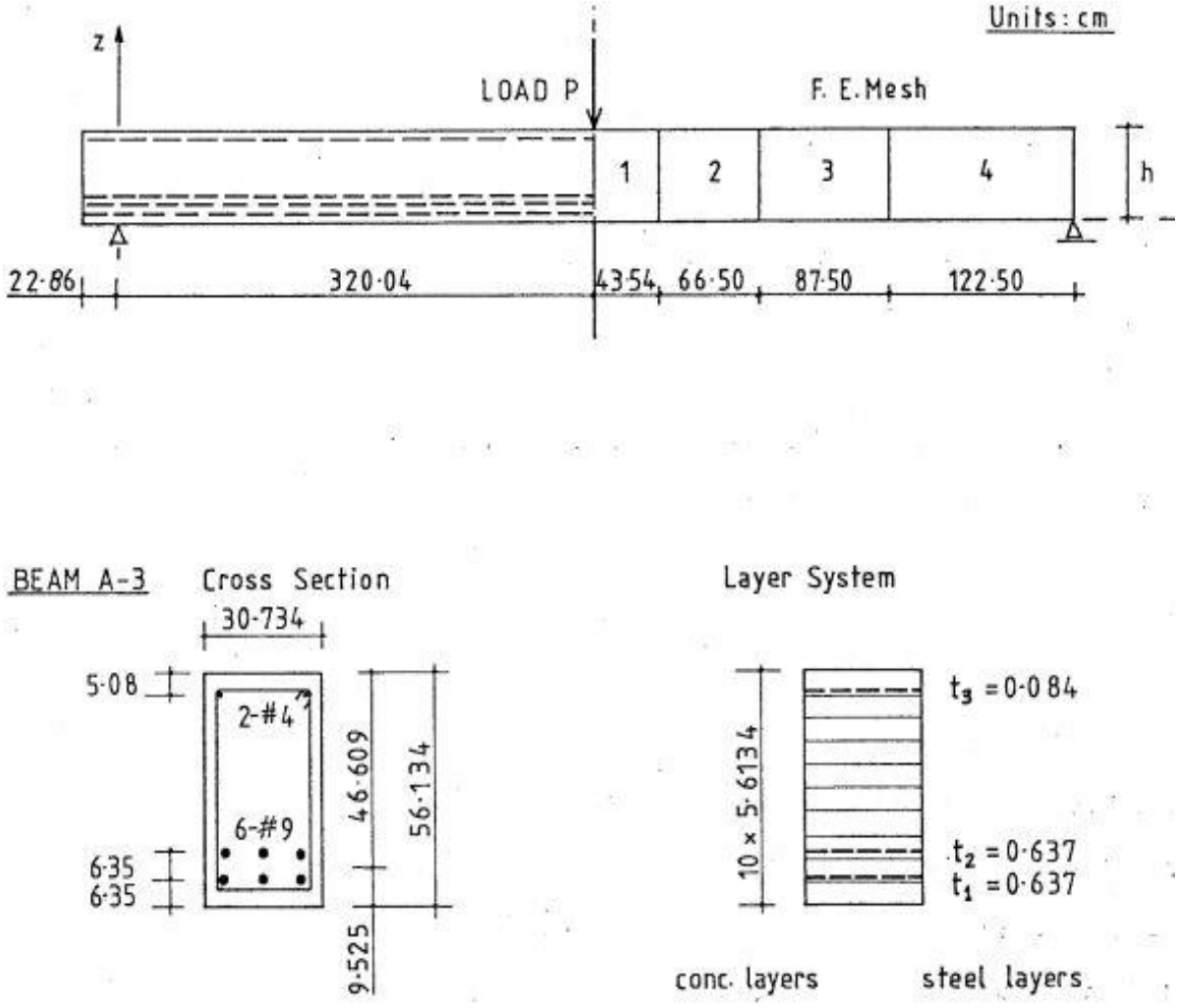

Figure 4.2: Geometry and Finite Element Idealization for Single Span Beam.

Table 4.1: Problem Parameters for Single Span Beam.

Material Properties (kN, cm)		
Concrete	Steel	
Young's Modulus, E_c=2980	Young′s Modulus, E_s = 2053	#9
Poisson′s Ratio, V = 0.15	Young′s Modulus, E_s' = 8150	
Ult. Comp. St., f′c = 3.50	Yield Stress, fy = 55.2	
Ult. Tens. St., ft′ = 0.43	Angle with x-axis, $\ominus$ =0.0	
Ult. Comp. St n., $\in$=0.003	Young′s Modulus, E_s = 20120	#4
Tens. Stiff. Coefficient, a = 0.6 (*)	Young′s Modulus, E_s' = 0	
Tens. Stiff. Coefficient, $\in_m$= 0.0015 (*)	Yield Stress, fy = 34.52	
(*) Only considered in the four bottom layers	Angle with x-axis, $\ominus$ =0.0	

4.2.2 Two Span Beam

The second structure is a two-span reinforced concrete beam with (80x60) mm^2 cross section area which has a (8Φ4) longitudinal reinforcement for compression and tension regions. The analysis of geometry and loading of the reinforced concrete beam (micro concrete) is illustrated in Figure 4-3 (a). Only one half of the beam is taken into consideration in the investigation due to symmetry. The same figure also includes the assumed loading and boundary conditions. The material properties of the beam are specified in Table 4-2, with identical steel properties and slightly different properties for concrete. The Young's modulus, E_c, the ultimate compressive stress, f_c' and the compressive strain at peak stress ($\in_C$=0.0027) were experimentally obtained. The other concrete properties have been assumed for the analysis.

a-

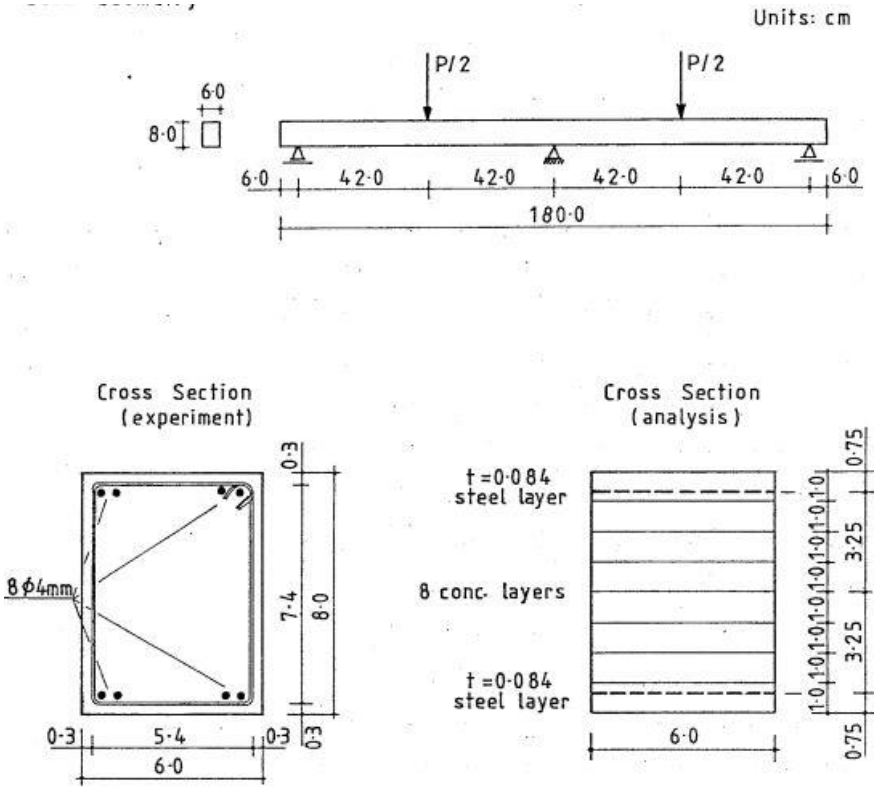

b-

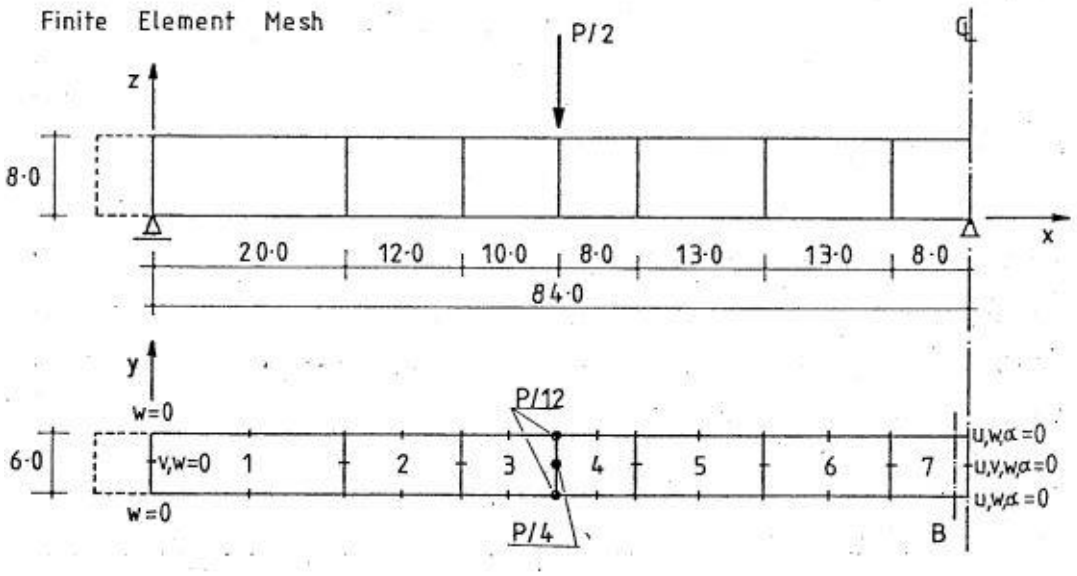

Figure 4.3: a- Geometry, b- Loading and Finite Element Idealization for Two Span Beam.

Table 4.2: Problem Parameters for Two Span Beam.

Material Properties (kN, cm)	
Concrete	Steel
Young's Modulus, E_c=1666	Young′s Modulus, E_s = 19600
Poisson′s Ratio, V = 0.0	Young′s Modulus, E_s' = 2800
Ult. Comp. St., f′c = 3.2	Young′s Modulus, E_s' '= 500
Ult. Tens. St., ft′ = 0.32	Yield Stress, fy = 49.0
Ult. Comp. St n., ϵ=0.004	Yield Stress, fy ' = 57.4
Tens. Stiff. Coefficient, a = 0.5	Angle with x-axis, θ =0.0
Tens. Stiff. Coefficient, ϵ_m= 0.0015	

4.2.3 One-Story Frame Building

The third structure is a one-story reinforced concrete frame which consist of two columns and a beam with a (250x150) mm^2 cross-section area, it has a (4Φ14) longitudinal reinforcement for both compression and tension regions. The geometry and loading of the reinforced concrete frame under analysis are illustrated in Figure 4-4. The material properties of the beam are specified in Table 4-3, with identical steel properties and slightly different properties for concrete. The 28-day compressive strength and the elastic modulus of the concrete were 27 MPa and 33 GPa, respectively. The longitudinal and stirrups bars have yield stresses of 448 and 433 MPa, respectively. The steel reinforcements' elastic modulus was 200 GPa. The distance between the clear concrete cover and the longitudinal bars was 20 mm. On the tops of the two columns, vertical point loads of 150 kN were applied. At one-third and two-thirds from the beam's left end, point loads of 12 kN were applied, which depicts the finite element mesh with the idealized planar stress.

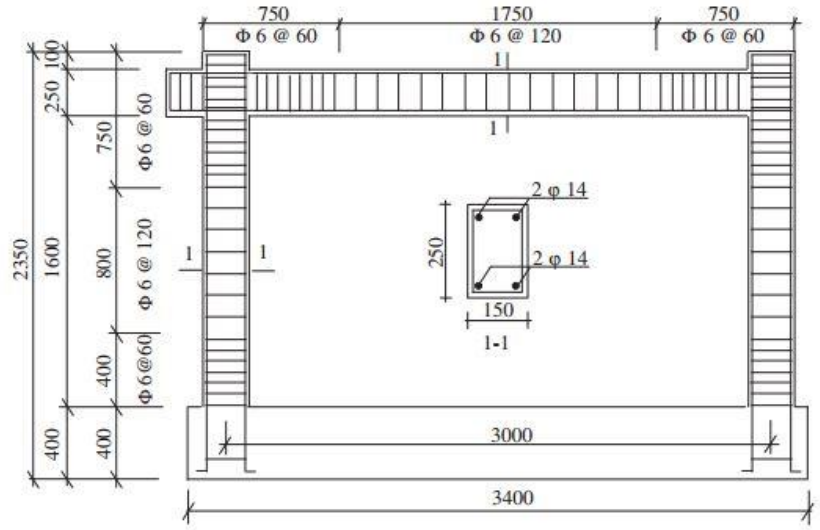

Figure 4.4: Details of The One-Story Frame.

Table 4.3: Problem Parameters for One Story Frame.

Material Properties (N, mm)	
Concrete	Steel
Young's Modulus, E_c=33000	Young′s Modulus, E_s = 200000
Ult. Comp. Strength, f'_c =27	Yield Stress for Longitudinal, fy = 448
	Yield Stress for Stirrups, fy = 433

4.3 Comparison of Load-Displacement Curves Results

This section presents the verification and numerical simulation results by presenting the load deflection curves for each of the previous structures. The numerical results and the experimental results have a good with acceptable correlation.

4.3.1 Single Span Beam

Figure 4-5 shows mid-span deflections against the total applied load. The experimental curve is compared with the numerical results. The findings of the experimental and SAP2000 verification are in good agreement. According to the results of the SAP2000 verification model, the collapse load (P=480 kN) is higher, and the reaction is stiffer at high loads. The load deflection curve due to numerical analysis has a more stiffened behavior, this can be attributed to the initial stiffness procedure adopted by SAP2000.

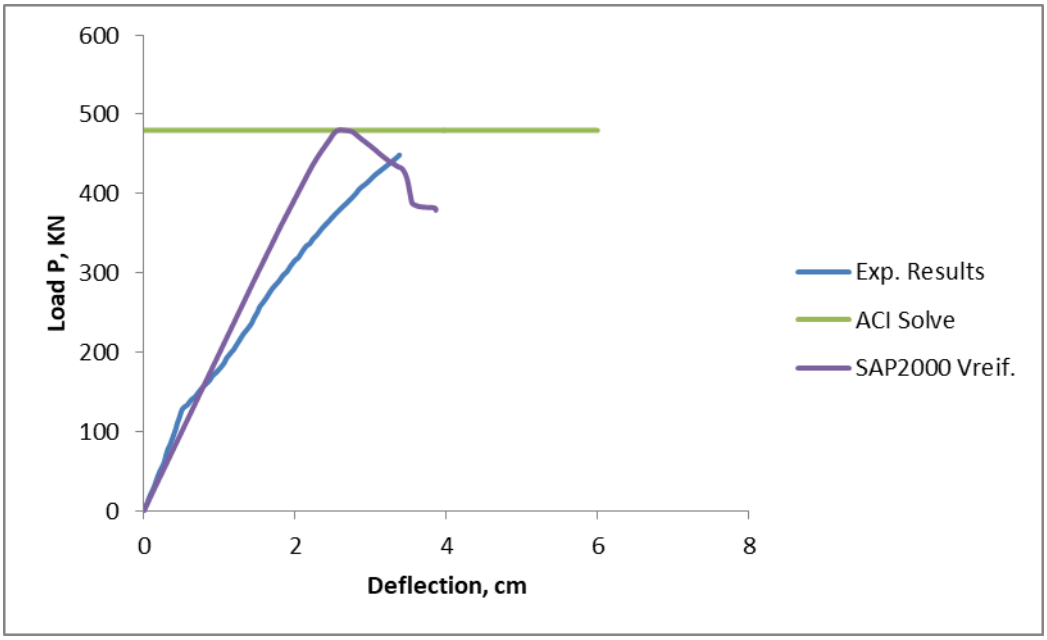

Figure 4.5: Load-Deflection Curve for Single Span Beam.

4.3.2 Two Span Beam

Figure 4-6 shows the point load deflection versus the total applied force. Using the same material parameters and concrete strength, the experimental results are compared to that of the numerical model. The numerical and the experimental results are in a good agreement. The ultimate load (Pu= 32.4 kN) is higher than the limit load suggested by the plastic hinge solution (Pu= 31.3 kN) and agrees with the experimental limit load. The initial stiffness method adopted by SAP2000 effects the nonlinear behavior of the structure, which makes the load deflection curve more stiffned.

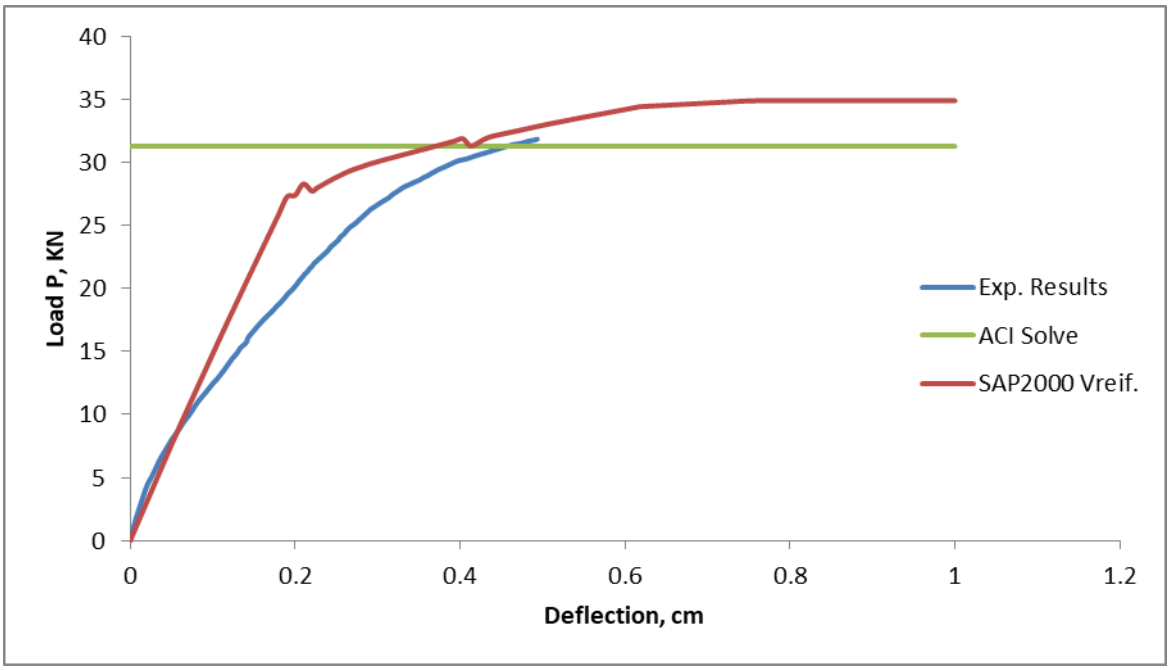

Figure 4.6: Load-Deflection Curve for Two Span Beam.

The ultimate strength for the numerical and the experimental results are close to the section analysis method according to the ACI code.

4.3.3 One-Story Frame Building

Fig.4-7 compares test results with the lateral load-displacement curve at the roof of the frame as predicted by a finite element model using nonlinear analysis by SAP2000 computer program. The agreement between the predictions and the observed data is depicted in this figure. For base shear force values between zero and 20 kN, the projected curve matches the observed curve. The stiffened behavior of the frame could be attributed to the initial stiffness method adopted by SAP2000.

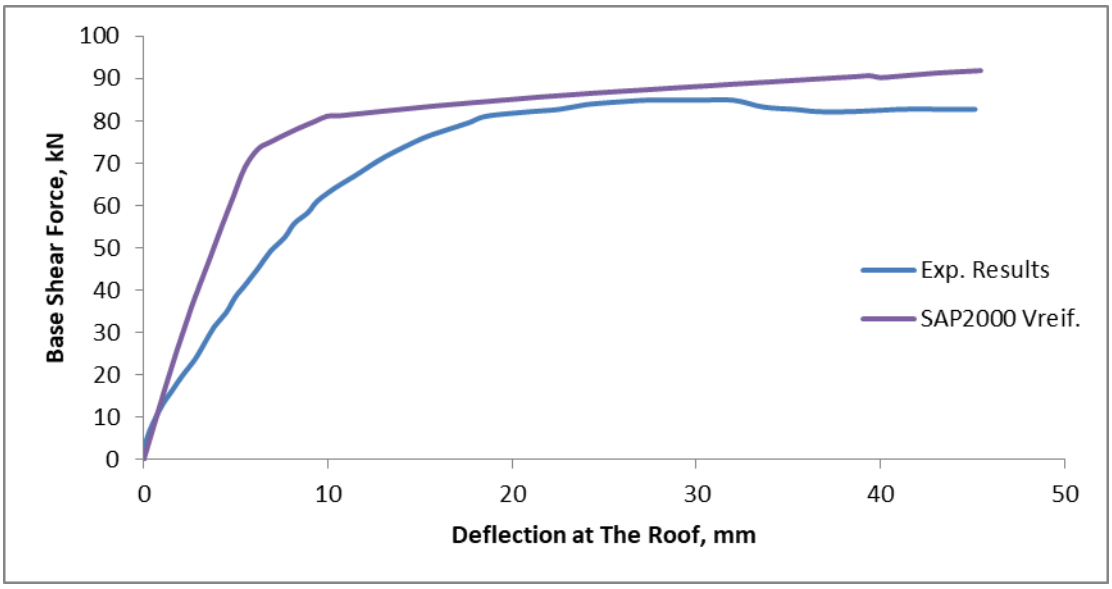

Figure 4.7: Load-Deflection Curve for One Story Frame.

CHAPTER 5: INTERMEDIATE MOMENT RESISTING FRAME MODELING AND CALIBRATION

5.1 Chapter Layout

In the present study the analytical and parametric study is conducted using the Finite Element Modeling Software SAP2000. To align with the expected behavior of a reinforced concrete building frame (comprising beams and columns) across various numbers of stories under ideal boundary conditions, the frame elements were modeling utilizing the SAP2000 software. This chapter explains the performance of frame elements using the Nonlinear Fiber Hinges Analysis Method. It also delves into concepts linked to and influenced by the response modification factor, such as ductility, overstrength factors, maximum lateral displacement, performance point levels, and the impact of Mander's Model on the stress-strain curves of concrete. Notably, Mander's Model is incorporated within the SAP2000 software. The analyses preformed account for nonlinear material characteristics and anticipate second-order effects post-design while applying different values of the response modification factor (R).

5.2 Mander's Model

Extensive research has been conducted on the stress-strain relationship between unconfined and confined concrete over the years. This section provides a brief overview of the models that are considered important for the present study.

5.2.1 Unconfined Concrete

A stress-strain equation for both confined and unconfined concrete was laid out by (Kent and Park in 1971). To more accurately explain the post-peak stress-strain behavior, they generalized (Hognestad's 1951) equation. The ascending branch is represented in this model by altering the Hognestad second-degree parabola by substituting $0.85f'_c$ by f'_c and $\mathcal{E}_{co}$ by 0.002.

$$f_c = f'_c \left[\frac{2\mathcal{E}_c}{\mathcal{E}_{co}} - \left(\frac{\mathcal{E}_c}{\mathcal{E}_{co}}\right)^2\right] \quad (4)$$

The post-peak branch was thought to be a straight line with a slope that was mostly determined by the strength of the concrete.

$$f_c = f'_c[1 - Z(\mathcal{E}_c - \mathcal{E}_{co})] \quad (5)$$

In which

$$Z = \frac{0.5}{\mathcal{E}_{50u} - \mathcal{E}_{co}} \quad (6)$$

Where $\mathcal{E}_{50u}$ = the strain corresponding to the stress equal to 50% of the maximum concrete strength for unconfined concrete

$$\mathcal{E}_{50u} = \frac{3 + 0.29f'_c}{145f'_c - 1000} \ (f'_c \ in \ MPa) \quad (7)$$

$$\mathcal{E}_{50u} = \frac{3 + 0.002f'_c}{f'_c - 1000} \ (f'_c \ in \ Psi) \quad (8)$$

Figure 5-1 represents the Kent and Park model.

To characterize the stress-strain behavior of unconfined concrete, (Popovics, 1973) suggested a single equation had been modified by (Thorenfeldt et al., 1987) and get generalized form of it by (Tsai, 1988).

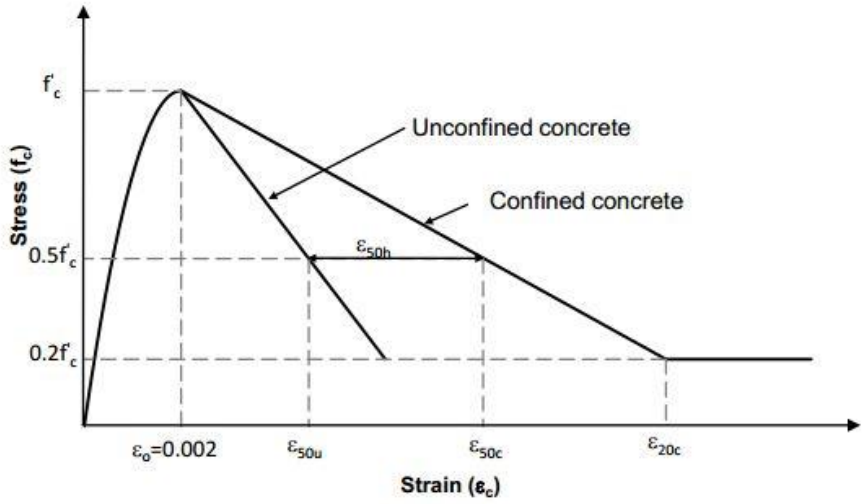

Figure 5.1: Proposed Stress-Strain Model for Confined and Unconfined Concrete – Kent And Park (1971) Model.

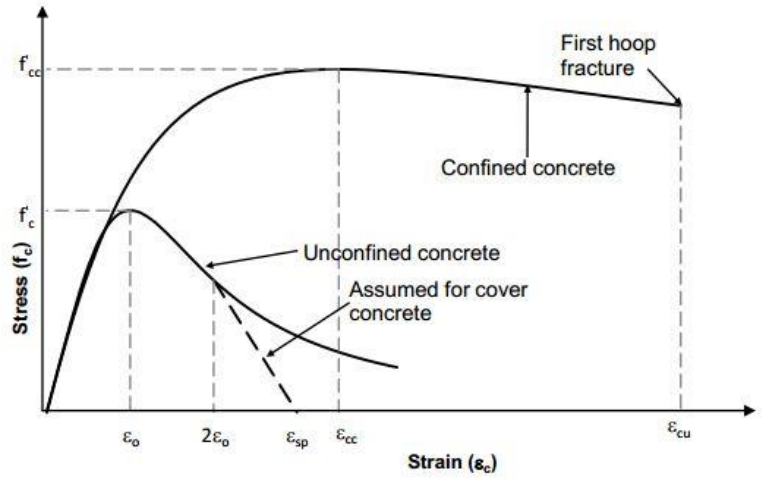

Figure 5.2: Stress-Strain Relation for Monotonic Loading of Confined and Unconfined Concrete - Mander Et Al. (1988b).

5.2.2 Confined Concrete

(Mander et al., 1988a) performed the first seismic strain rate tests on full size circular, rectangular, and square columns to examine the effects of various transverse reinforcement arrangements on confinement efficacy and overall performance. (Mander et al., 1988b) then modeled the outcomes of their experiments. It was found that, regardless of how the confinement reinforcement was arranged, performance across the whole stress-strain range was comparable if the peak strain and stress coordinates could be identified. In order to create a generalized multi-axial confinement model, they therefore selected a failure criterion based on a 5-parameter model of (William and Warnke, 1975) and data from (Schickert and Winkler, 1979). In order to fully explain the stress-strain curve, they then used (Popovics', 1973) three-parameter equation. The equations are shown in Figure 5-2.

$$\frac{f_c}{f'_{cc}} = \frac{n\left(\frac{\varepsilon_c}{\varepsilon_{cc}}\right)}{(n-1)+\left(\frac{\varepsilon_c}{\varepsilon_{cc}}\right)^n} \tag{9}$$

In which

$$n = \frac{E_c}{E_c - E_{sec}} \tag{10}$$

$$E_c(MPa) = 5000\sqrt{f'_c(MPa)} \tag{11}$$

$$E_{sec} = \frac{f'_{cc}}{\varepsilon_{cc}} \tag{12}$$

$\mathcal{E}_{cc}$ is the strain at the maximum compressive strength of confined concrete f'_{cc}

$$\varepsilon_{cc} = \varepsilon_{co}\left[1 + 5\left(\frac{f'_{cc}}{f'_c} - 1\right)\right] \quad (13)$$

f'_{cc}, the compressive strength of confined concrete is given as

$$f'_{cc} = f'_c\left(-1.254 + 2.254\sqrt{1 + \frac{7.94f'_l}{f'_c}} - 2\frac{f'_l}{f'_c}\right) \quad (14)$$

In which f'_l is given by:

$$f'_l = \frac{1}{2}k_e\rho_s f_{yh} \quad (15)$$

In which ρ_s = ratio of volume of transverse confining steel to the volume of confined concrete core, f_{yh}= yield strength of transverse reinforcement, k_e = confinement coefficient.

For circular hoops: $$k_e = \frac{\left(1-\frac{s'}{2d_s}\right)^2}{1-\rho_{cc}} \quad (16)$$

For circular spirals: $$k_e = \frac{1-\frac{s'}{2d_s}}{1-\rho_{cc}} \quad (17)$$

where ρ_{cc} = ratio of area of longitudinal reinforcement to area of core of the section, s' = clear spacing between spiral or hoop bars, d_s = diameter of spiral.

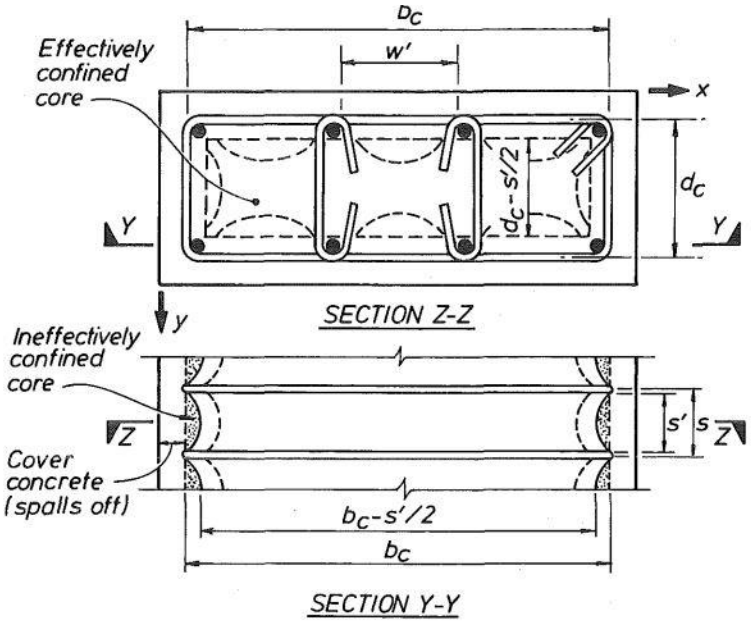

Figure 5.3: Effectively Confined Core for Rectangular Hoop Reinforcement.

For rectangular hoops with or without cross ties, Figure 5-3, it is once more assumed that the arching action will take the shape of second-degree parabolas with a 45° starting tangent slope. Arching happens between layers of transverse hoop bars vertically and between longitudinal bars horizontally. Subtracting the area of the parabolas containing the ineffectively contained concrete yields the area of concrete that is effectively confined at hoop level. According to Figure 5-3, the ineffective area for a single parabola is $(w'_i)^2/6$, where w'_i is the i-th clear distance between neighboring longitudinal bars. Therefore, when there are n longitudinal bars, the total plan area of ineffectively confined core concrete at the level of the hoops is:

$$A_i = \sum_{i=1}^{n} \frac{(w'_i)^2}{6} \tag{18}$$

The area of successfully restricted concrete core at the midpoint between the levels of transverse hoop reinforcement is calculated by factoring in the influence of the ineffective portions in the elevation Figure 5-3.

$$A_e = \left(b_c d_c \sum_{i=1}^{n} \frac{(w'_i)^2}{6}\right)\left(1 - \frac{s'}{2b_c}\right)\left(1 - \frac{s'}{2d_c}\right) \tag{19}$$

Where b_c and d_c = core dimension to the centerline of perimeter hoop in x and y direction, respectively, where $b_c > d_c$. Also, the area of concrete core enclosed by the perimeter hoops is given by Eq. 18. Hence from Eq. 17 the confinement effectiveness coefficient is for rectangular hoops.

$$k_e = \frac{A_e}{A_{cc}} \tag{20}$$

Where k_e = confinement effective coefficient, A_e = area of effectively confined concrete core.

$$A_{cc} = A_c(1 - \rho_{cc}) \tag{21}$$

ρ_{cc} = ratio of area of longitudinal reinforcement to area of core of section, and A_c = area of core of section enclosed by the center lines of the perimeter spiral or hoop.

$$k_e = \frac{\left(1 - \sum_{i=1}^{n} \frac{(w'_i)^2}{6}\right)\left(1 - \frac{s'}{2b_c}\right)\left(1 - \frac{s'}{2d_c}\right)}{1 - \rho_{cc}} \quad (22)$$

In the x and y dimensions, rectangular reinforced concrete members may have varying amounts of transverse confining steel. These could be stated as:

$$\rho_x = \frac{A_{sx}}{sd_c} \quad (23)$$

And

$$\rho_y = \frac{A_{sy}}{sb_c} \quad (24)$$

Where A_{sx} and A_{sy} = the total area of transverse bars running in the x and y direction, respectively (see Figure 5-3).

The lateral confining stress on the concrete (total transverse bar force divided by vertical area of confined concrete) is given in the x direction as:

$$f_{lx} = \frac{A_{sx}}{sd_c} f_{yh} = \rho_x f_{yh} \quad (25)$$

And in y direction as:

$$f_{ly} = \frac{A_{sy}}{sb_c} f_{yh} = \rho_y f_{yh} \quad (26)$$

From Eq. 25 and 26 the effective lateral confining stresses in the *x* and y directions are:

$$f'_l = f_l k_e \quad (27)$$

Where f_l = lateral pressure from the transverse reinforcement, assumed to be uniformly distributed over the surface of the concrete core.

$$f'_{lx} = \rho_x f_{yh} k_e \quad (28)$$

And

$$f'_{ly} = \rho_y f_{yh} k_e \quad (29)$$

Where k_e is given in Eq. 22.

The Mander et al. (1988b) model has been widely used in design and research due of its generality. Despite this, it has a number of drawbacks. Since the initial tests were created

in the 1980s, the use of high performance (strength) materials, particularly high strength concrete, has increased significantly. The Mander et al. (1988b) model needs to be modified because it does not effectively handle the post-peak branch of high strength concrete.

5.3 Ductility Factor (μ)

Displacement capacity, ductility, and ductility ratio are earthquake response statistics that are interconnected yet frequently misunderstood. As an instance, a frame with a high displacement capacity may have low ductility and a low ductility ratio, whereas a frame with a low displacement capacity may have high ductility but low ductility ratio. At the elemental, stories, and system levels, the ductility ratio (μ) can be computed. The ductility ratio is typically expressed in terms of the displacement ductility ratio at the story levels and system. The curvature, strain, and rotation ductility ratios are three ways to express ductility ratio at the elemental level. To calculate the ductility factor, displacement ductility ratio was employed.

The hysteretic energy-induced nonlinear response of a structure was calculated using the reduction factor given to R. R is dependent on the parameters of the ground motion during an earthquake as well as structural qualities including damping, ductility, and the basic period of vibration. The idealized yielding point (Δ_y), created by (Newmark and Hall, 1982), corresponds to the maximum structural drift (Δ_{max}), which is how R is expressed in Eq. (30-32):

$$R_\mu = \mu \quad \text{if T} > 0.5 \text{ sec} \tag{30}$$

$$R_\mu = \sqrt{2\mu - 1} \quad \text{if } 0.1 < \text{T} < 0.5 \text{ sec} \tag{31}$$

$$R_\mu = 1 \quad \text{if T} < 0.03 \text{ sec} \tag{32}$$

Where T is the fundamental period and μ is the displacement ductility factor defined as follow in Eq. (33):

$$\mu = \frac{\Delta_{max}}{\Delta_y} \tag{33}$$

Where Δ_{max} is the maximum displacement (displacement corresponding to the limit state), and Δ_y is the yield displacement of the structure.

5.4 Over Strength Code Factor (Ω)

Structures are typically originally designed using equivalent static forces defined by building codes. These static forces are divided inherently based on fundamental elastic vibration modes. Since it is impossible to attain full safety and sturdiness during construction, current structural design codes an earthquake having a decent chance of happening (ATC3-06, 1978). However, by using an inelastic energy dissipation system, a number of structural and nonstructural damages can be analyzed to economically attain a high level of safety in structural design. The majority of seismic codes allow a decrease in design loads by stating that structures have a sizable amount of reserve strength (over-strength Ω) and the ability to disperse energy (ductility$R\mu$). R combines these characteristics in its structural architecture (Kim et al., 2005). When designing for lateral strength, lateral strength is often less than what seismic standards specify is necessary for structures to remain elastic.

Calculating the actual forces acting on a structural element designed to remain elastic involves taking into account an over-strength factor in seismic design. For tall buildings, the sources that contribute to this over-strength have not yet been extensively quantified (Khy K et.al., 2019). Even if the earthquake's actual seismic demands exceeding their design values, most of buildings with shear wall structures perform well and appear to sustain little to no damage (L. M. Massone et.al. 2012 and D. Ugalde and D. Lopez-Garcia, 2017). This is because the design's essential reserve strength or over-strength, which keeps structures from collapsing. The ratio of actual ultimate lateral strength to code-based design lateral force is known as the over-strength factor (Ω). The provisions of (ASCE 7-16, 2016 and NBCC, 2010) acknowledge the existence of a building's significant over-strength.

While the over-strength factor is implicitly taken into account in (ASCE 7-16, 2016) with the usage of response modification factor (R), which represents both ductility and over-strength factors, the over-strength component is explicitly shown in (NBCC, 2010) as an over-strength related force modification factor (R_0). When designing critical structural members that must remain essentially elastic, such as collectors in a diaphragm, transfer beams, discontinuous systems, and elements supporting discontinuous frames or walls, the over-strength factor plays a key role in amplifying seismic forces (ASCE 7-16, 2016).

Because it can enhance the shear forces of RC shear walls, the over-strength factor is also connected to the shear-amplification issue in shear walls (K. Khy et.al., 2019 and K. Leng et.al., 2014). To calculate the design forces of certain structural elements, it is crucial to estimate the over-strength factor accurately.

A building over strength can be attributed to a variety of factors that have all been extensively discussed in several earlier research (C. M. Uang, 1991and A. S. Elnashai and A. M. Mwafy, 2002). Two categories can be used to categorize various factors that contribute to the over-strength factor (ASCE 7-16, 2016 and C. M. Uang, 1991and). Material over-strength (actual material strengths are higher than nominal strengths specified in design), strength reduction factor (Φ), multiple load cases and load combinations, conservative design selection (selecting sections or specifying reinforcements that exceed the required design), design controlled by code minimum requirement, and design controlled by drift rather than strength are among the factors in the first group that contribute to the design process. The second group has to do with redundancy (the redistribution of internal forces among structural parts following the occurrence of yielding) and steel strain-hardening.

According to Figure 5-4, the whole over-strength factor (Ω) is divided into two categories. The first type is the so-called first-yield over-strength factor (Ω_1), which is the relationship between the design base shear force (V_d) and the first-yield lateral strength (V_{fy}), as indicated in Eq. (34). The second kind of over-strength results from internal force redistribution and steel strain hardening (Ω_2), which is the ratio between ultimate lateral strength (V_{ult}) and first-yield lateral strength, as indicated in Eq. (35). According to Eq. (36), the ratio between the ultimate lateral strength and the design base shear force is the total over-strength factor.

$$\Omega 1 = \frac{Vfy}{Vd} \quad (34)$$

$$\Omega 2 = \frac{Vult}{Vfy} \quad (35)$$

$$\Omega = \Omega 1 \text{x } \Omega 2 = \frac{Vult}{Vd} \quad (36)$$

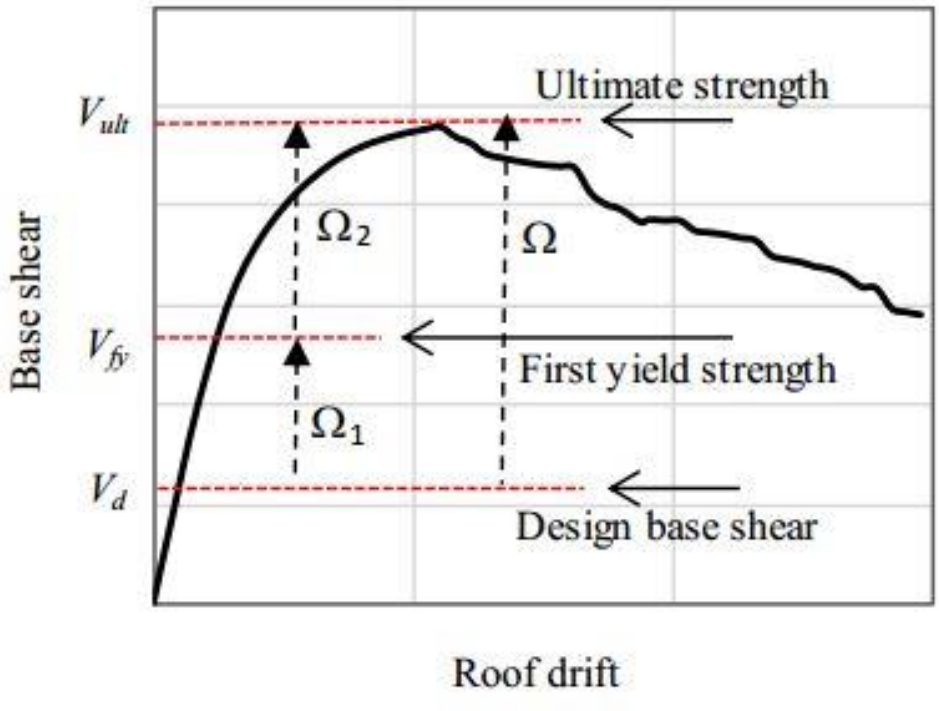

Figure 5.4: Lateral Load Capacity Curve and Over-Strength Factor of The Building.

5.5 Performance Point and Performance Level of Structures Against Earthquakes

The performance point is the point on the pushover curve with the greatest seismic displacement. Utilizing data obtained from the pushover analysis, engineers can assess the structural condition aligned with the displacement of this performance point. This assessment aids in locating plastic hinges, gauging their limit states, and determining inter-story drifts. In other words, it signifies the point of physical equilibrium between structural capacity and seismic demand. The pushover curve, or capacity curve, represents the structural capacity, while the acceleration response spectrum of ground motions, or demand curve, signifies seismic demand, as shown in Figure 5-5. In theory, the performance point is the point at which the capacity and demand curves intersect. However, the capacity curve is represented as force versus displacement, while the demand curve is expressed as spectral acceleration versus period. To establish a common performance point, these two curves must initially be standardized to the same reference frame (Pednekar SC et al., 2015).

The Acceleration Displacement Response Spectra (ADRS) is a standardized reference that illustrates the relationship between spectral acceleration and spectral displacement. The spectral accelerations and displacements corresponding to the base shear forces and control node displacements of the capacity curve are calculated utilizing structural modal traits (i.e., modal mass and modal participation factor), and the capacity spectrum in the ADRS form is obtained. The equivalent spectral displacements can be calculated using the spectral accelerations and associated periods of the demand curve, and the demand spectrum in the ADRS form can be generated. Finding the performance point is not an easy task once the capacity and demand curves are given in the ADRS form. In fact, the first acceleration response spectrum (demand curve) corresponds to an elastic structure with a damping factor of about 5%. While plastic deformations occur in the structure, hysteretic damping is generated, increasing the overall damping of the structure.

To calculate the performance point ATC40 method is adopted. Advance Design can now determine the performance point using either method (Dal Lago B and Molina FJ, 2018).

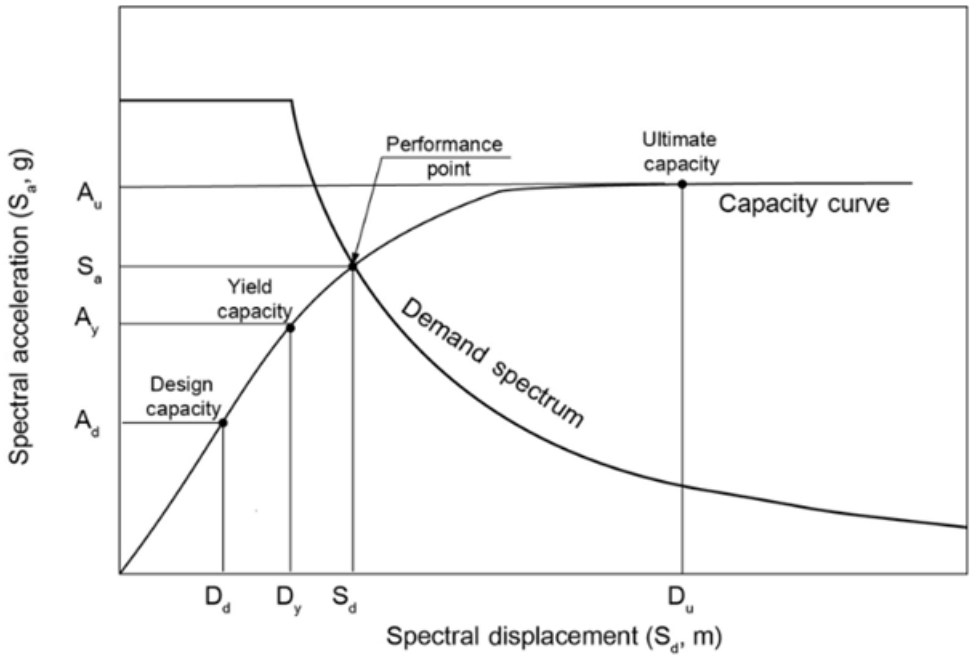

Figure 5.5: Performance Point Curve.

Upon determining the performance point, the structure's performance is evaluated to four levels of earthquake resistance: Operational Performance Level (OP), Immediate Occupancy Performance Level (IO), Life Safety Performance Level (LS), and Collapse Prevention Performance Level (CP).

Immediate Occupancy Performance Level (IO) signifies a scenario where the structure sustains minor damage. There's no significant permanent drift, maintaining the original strength and stiffness. Minor cracking might occur in facades, partitions, ceilings, and structural elements, with the building's space and systems generally being fairly usable. Equipment and contents are generally secure, although they may not function due to mechanical failure or utility disruptions. Concrete frames experience minor hairline cracking, limited yielding in a few locations, and no excessive deformation (strain of concrete less than 0.003). Steel moment frames exhibit minor local yielding in specific locations, with no buckling, fractures, or noticeable distortions of members. In braced steel frame structures, minor yielding or distortion of braces might occur.

Life Safety Performance Level (LS) aims to achieve a damage condition with a low probability of endangering life safety. Moderate overall damage is evident, yet all stories retain residual strength and stiffness. No out-of-plane wall failures or parapet tipping occurs. However, permanent drift is present, and partitions suffer damage. The building may be beyond economical repair, and while falling hazards are mitigated, numerous architectural, mechanical, and electrical systems sustain damage. Concrete frame beams suffer extensive damage, exhibiting shear cracking and spalling of cover in ductile columns, along with minor cracking in nonductile columns. Hinges form in steel moment frames, accompanied by local buckling of some beams, significant joint distortion, and isolated moment connection fractures. Despite this, shear connections remain sound, and few elements may partially fracture. In braced frames, most braces yield or buckle to some extent, and certain connections might fail.

Collapse Prevention Performance Level (CP) mainly concerns the vertical load-carrying system, requiring the structure to remain stable under vertical loads only. Typically, building damage is severe, and residual stiffness and strength are minimal. While load-bearing columns and walls continue to function, substantial permanent drifts occur, some exits might be blocked, and infills and unbraced parapets either fail or are on the verge of failure. The building nears collapse, nonstructural components suffer extensive damage, hinges and extensive cracking arise in ductile elements of concrete frames, nonductile columns experience splice failure and limited cracking, and short columns are significantly damaged. In steel frames, beams and columns undergo pronounced distortion, while several moment connections fracture, and shear connections stay intact. In braced frames, numerous braces yield and buckle extensively, with many of them, along with their connections, facing potential failure, as shown in Figure 5-6.

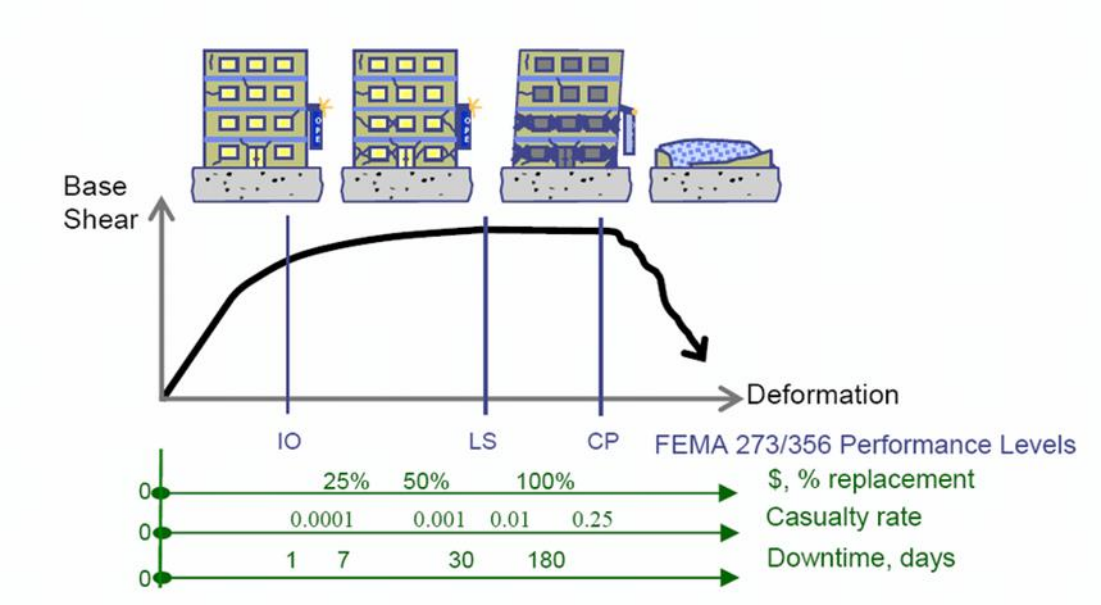

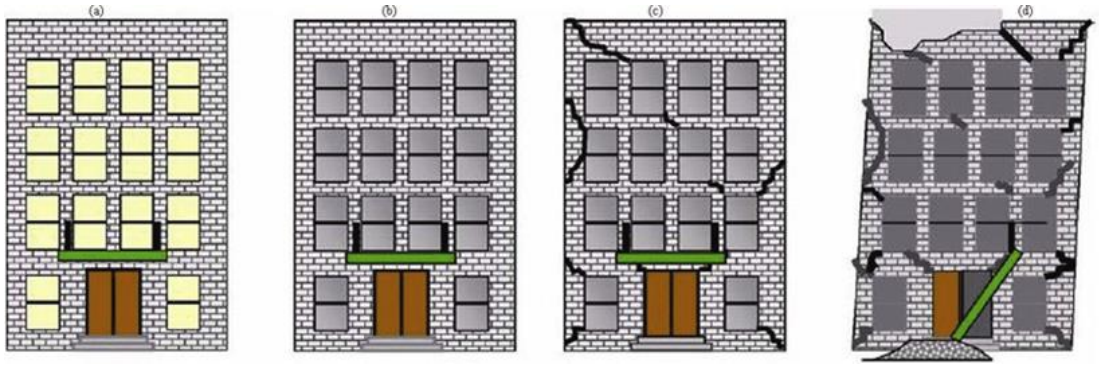

Figure 5.6: Levels of Building Performance: (A) Operational, (B) Immediate Occupancy, (C) Life-Safety, And (D) Collapse Prevention.

5.6 Design of the Intermediate Moment Resisting Frame

In order to determine the design and details of the intermediate concrete moment resisting frame which described in CHAPTER 3, the ACI-318 (18-4) equations were used after to get the value of the ultimate bending moment from ETABS18.1.1 which resulted from the following code load combinations as follow in Eq. (37-40).

$1.4\ DL.$ (37)

$1.2\ DL + 1.6\ LL.$ (38)

$(1.2 + 0.2S_{DS})DL + 1.0LL + 1.3Q_{E.}$ (39)

$(0.9 - 0.2S_{DS})DL + 1.3Q_{E.}$ (40)

Check the limitation section dimension Eq. (41-42):

$\frac{L_n}{d} > 4\ NOT\ DEEPBEAM$ (41)

$\frac{b}{h} > 0.3\ OK$ (42)

Design procedure Eq. (43-46):

$K_n = \frac{M_u/\emptyset}{bd^2}$ (43)

$m = \frac{f_y}{0.85f'_c}$ (44)

$\rho = \frac{1}{m}\left(1 - \sqrt{1 - \frac{2mK_n}{f_y}}\right)$ (45)

$As_{req} = \rho bd$ (46)

Check minimum area of steel and strain Eq. (47-48):

$$As_{min} = \frac{1.4}{f_y} bd > 0.25 \frac{\sqrt{f'_c}}{f_y} \quad (47)$$

$$\varepsilon = \frac{d-c}{c} 0.003 > 0.005 \quad (48)$$

According to the previous equations, the design of the reinforced concrete frame is explained in Table 3-2.

Following the same procedure, the same frame has been designed at different values of the response modification factor (R) than those specified from ASCE7-16 Code (R = 1,2,3,4,5,6 and 7), to study its impact on the design of one-story building (ground floor) which explained in Tables ((5-1)- (5-7)) therefore the nominal bending moment and strength of the frame after getting the analysis study.

Table 5.1: Design of The Reinforced Concrete Frames, per ACI-318 (18.4) For R=1

The edge frames (1, 4 and in the other direction A, E) reinforcement for R=1					
Location		As required (mm^2)	Reinforcement	ΦMn (kN.m)	Mn (kN.m)
End Span	Left	2701	7Φ22	352.2	414.4
		2188	6Φ22	308.6	363.1
	Right	2657	7Φ22	352.2	414.4
		1680	6Φ22	308.6	363.1
Mid Span	Left	2365	7Φ22	352.2	414.4
		1522	6Φ22	308.6	363.1
	Right	2345	7Φ22	352.2	414.4
		1574	6Φ22	308.6	363.1
The mid frames (2, 3 and in the other direction B, C, D) reinforcement for R=1					
Location		As required (mm^2)	Reinforcement	ΦMn (kN.m)	Mn (kN.m)
End Span	Left	3063	8Φ22	393.5	462.9
		2147	6Φ22	308.6	363.1
	Right	3198	8Φ22	393.5	462.9
		1460	6Φ22	308.6	363.1
Mid Span	Left	2668	8Φ22	393.5	462.9
		1289	6Φ22	308.6	363.1
	Right	2786	8Φ22	393.5	462.9
		1399	6Φ22	308.6	363.1

ΦMn(+ve) > ΦMn(-ve)/3 OK.

Table 5.2: Design of The Reinforced Concrete Frames, per ACI-318 (18.4) For R=2

The edge frames (1, 4 and in the other direction A, E) reinforcement for R=2					
Location		As required (mm^2)	Reinforcement	ΦMn (kN.m)	Mn (kN.m)
End Span	Left	1356	6Φ18	215.2	239.1
		1032	6Φ12	100.3	111.4
	Right	1522	6Φ18	215.2	239.1
		646 use Min 675	6Φ12	100.3	111.4
Mid Span	Left	1334	6Φ18	215.2	239.1
		640 use Min 675	6Φ12	100.3	111.4
	Right	1287	6Φ18	215.2	239.1
		640 use Min 675	6Φ12	100.3	111.4
The mid frames (2, 3 and in the other direction B, C, D) reinforcement for R=2					
Location		As required (mm^2)	Reinforcement	ΦMn (kN.m)	Mn (kN.m)
End Span	Left	1558	8Φ18	278.9	309.9
		978	5Φ14	113.3	125.9
	Right	2015	8Φ18	278.9	309.9
		736	5Φ14	113.3	125.9
Mid Span	Left	1633	8Φ18	278.9	309.9
		691	5Φ14	113.3	125.9
	Right	1649	8Φ18	278.9	309.9
		640 use Min 675	5Φ14	113.3	125.9

ΦMn(+ve) > ΦMn(-ve)/3 OK.

Table 5.3: Design of The Reinforced Concrete Frames, per ACI-318 (18.4) For R=3

The edge frames (1, 4 and in the other direction A, E) reinforcement for R=3					
Location		As required (mm^2)	Reinforcement	ΦMn (kN.m)	Mn (kN.m)
End Span	Left	948	6Φ16	173.3	192.6
		640 use Min 675	6Φ12	100.3	111.4
	Right	1173	6Φ16	173.3	192.6
		640 use Min 675	6Φ12	100.3	111.4
Mid Span	Left	1033	6Φ16	173.3	192.6
		613 use Min 675	6Φ12	100.3	111.4
	Right	980	6Φ16	173.3	192.6
		588 use Min 675	6Φ12	100.3	111.4
The mid frames (2, 3 and in the other direction B, C, D) reinforcement For R=3					
Location		As required (mm^2)	Reinforcement	ΦMn (kN.m)	Mn (kN.m)
End Span	Left	1131	7Φ18	247.6	275.1
		741	6Φ12	100.3	111.4
	Right	1642	7Φ18	247.6	275.1
		640 use Min 675	6Φ12	100.3	111.4
Mid Span	Left	1433	7Φ18	247.6	275.1
		640 use Min 675	6Φ12	100.3	111.4
	Right	1333	7Φ18	247.6	275.1
		640 use Min 675	6Φ12	100.3	111.4

ΦMn(+ve) > ΦMn(-ve)/3 OK.

Table 5.4: Design of The Reinforced Concrete Frames, per ACI-318 (18.4) For R=4

The edge frames (1, 4 and in the other direction A, E) reinforcement for R=4					
Location		As required (mm^2)	Reinforcement	ΦMn (kN.m)	Mn (kN.m)
End Span	Left	751	7Φ14	156	173.3
		640 use Min 675	6Φ12	100.3	111.4
	Right	1004	7Φ14	156	173.3
		614 use Min 675	6Φ12	100.3	111.4
Mid Span	Left	886	7Φ14	156	173.3
		542 use Min 675	6Φ12	100.3	111.4
	Right	830	7Φ14	156	173.3
		516 use Min 675	6Φ12	100.3	111.4
The mid frames (2, 3 and in the other direction B, C, D) reinforcement for R=4					
Location		As required (mm^2)	Reinforcement	ΦMn (kN.m)	Mn (kN.m)
End Span	Left	924	6Φ18	215.2	239.1
		640 use Min 675	6Φ12	100.3	111.4
	Right	1462	6Φ18	215.2	239.1
		640 use Min 675	6Φ12	100.3	111.4
Mid Span	Left	1278	6Φ18	215.2	239.1
		640 use Min 675	6Φ12	100.3	111.4
	Right	1176	6Φ18	215.2	239.1
		630 use Min 675	6Φ12	100.3	111.4

ΦMn(+ve) > ΦMn(-ve)/3 OK.

Table 5.5: Design of The Reinforced Concrete Frames, per ACI-318 (18.4) For R=5

The edge frames (1, 4 and in the other direction A, E) reinforcement for R=5					
Location		As required (mm^2)	Reinforcement	ΦMn (kN.m)	Mn (kN.m)
End Span	Left	663	6Φ14	134.8	149.8
		640 use Min 675	6Φ12	100.3	111.4
	Right	904	6Φ14	134.8	149.8
		566 use Min 675	6Φ12	100.3	111.4
Mid Span	Left	799	6Φ14	134.8	149.8
		500 use Min 675	6Φ12	100.3	111.4
	Right	741	6Φ14	134.8	149.8
		473 use Min 675	6Φ12	100.3	111.4
The mid frames (2, 3 and in the other direction B, C, D) reinforcement for R=5					
Location		As required (mm^2)	Reinforcement	ΦMn (kN.m)	Mn (kN.m)
End Span	Left	803	7Φ16	200	222.2
		640 use Min 675	6Φ12	100.3	111.4
	Right	1356	7Φ16	200	222.2
		640 use Min 675	6Φ12	100.3	111.4
Mid Span	Left	1187	7Φ16	200	222.2
		633 use Min 675	6Φ12	100.3	111.4
	Right	1084	7Φ16	200	222.2
		591 use Min 675	6Φ12	100.3	111.4

ΦMn(+ve) > ΦMn(-ve)/3 OK.

Table 5.6: Design of The Reinforced Concrete Frames, per ACI-318 (18.4) For R=6

The edge frames (1, 4 and in the other direction A, E) reinforcement for R=6					
Location		As required (mm^2)	Reinforcement	ΦMn (kN.m)	Mn (kN.m)
End Span	Left	640	6Φ14	134.8	149.8
		540 use Min 675	6Φ12	100.3	111.4
	Right	838	6Φ14	134.8	149.8
		534 use Min 675	6Φ12	100.3	111.4
Mid Span	Left	741	6Φ14	134.8	149.8
		477 use Min 675	6Φ12	100.3	111.4
	Right	683	6Φ14	134.8	149.8
		445 use Min 675	6Φ12	100.3	111.4
The mid frames (2, 3 and in the other direction B, C, D) reinforcement for R=6					
Location		As required (mm^2)	Reinforcement	ΦMn (kN.m)	Mn (kN.m)
End Span	Left	723	5Φ18	181.9	202.1
		640 use Min 675	6Φ12	100.3	111.4
	Right	1286	5Φ18	181.9	202.1
		640 use Min 675	6Φ12	100.3	111.4
Mid Span	Left	1127	5Φ18	181.9	202.1
		607 use Min 675	6Φ12	100.3	111.4
	Right	1023	5Φ18	181.9	202.1
		566 use Min 675	6Φ12	100.3	111.4

ΦMn(+ve) > ΦMn(-ve)/3 OK.

Table 5.7: Design of The Reinforced Concrete Frames, per ACI-318 (18.4) For R=7

The edge frames (1, 4 and in the other direction A, E) reinforcement for R=7					
Location		As required (mm^2)	Reinforcement	ΦMn (kN.m)	Mn (kN.m)
End Span	Left	640	4Φ16	118.1	131.2
		497 use Min 675	6Φ12	100.3	111.4
	Right	791	4Φ16	118.1	131.2
		511 use Min 675	6Φ12	100.3	111.4
Mid Span	Left	701	4Φ16	118.1	131.2
		452 use Min 675	6Φ12	100.3	111.4
	Right	648	4Φ16	118.1	131.2
		424 use Min 675	6Φ12	100.3	111.4
The mid frames (2, 3 and in the other direction B, C, D) reinforcement for R=7					
Location		As required (mm^2)	Reinforcement	ΦMn (kN.m)	Mn (kN.m)
End Span	Left	671	6Φ16	173.3	192.6
		640 use Min 675	6Φ12	100.3	111.4
	Right	1237	6Φ16	173.3	192.6
		640 use Min 675	6Φ12	100.3	111.4
Mid Span	Left	1084	6Φ16	173.3	192.6
		589 use Min 675	6Φ12	100.3	111.4
	Right	979	6Φ16	173.3	192.6
		547 use Min 675	6Φ12	100.3	111.4

ΦMn(+ve) > ΦMn(-ve)/3 OK.

CHAPTER 6: RESULTS AND DISCUSSION OF ANALYTICAL PARAMETEIC STUDY

6.1 Capacity Curve of IMRF

The first portion of the analysis results section will focus on the behavior of a one floor (ground floor) building with a reinforced concrete intermediate moment resisting frame (IMRF). This frame was proposed and described in CHAPTER-3, and its Design Conditions and Site Class Specific Factors are classified in Table 3-1. The building is subjected to a presumed earthquake while different values of the response modification factor R, ranging from 1 to 7, are used. The design details are explained in the previous chapter in Tables (5-1) to (5-7).

For each value of R, a capacity curve (Load-Displacement Curve) is plotted for the frame structure, as shown in Figure 6-1. In this case, the base shear is 3144 kN, the importance factor according to ASCE 7-16 code is 1.25, the earthquake's redundancy factor ($\rho = 1.3$), and the thickness of the two-way solid slab is 250 mm.

Figures (6-2) and (6-3) show the behavior of the same frames with same previous conditions but with different number of stories (first and second floor). The base shear for these cases is 6382 kN and 9522 kN, respectively.

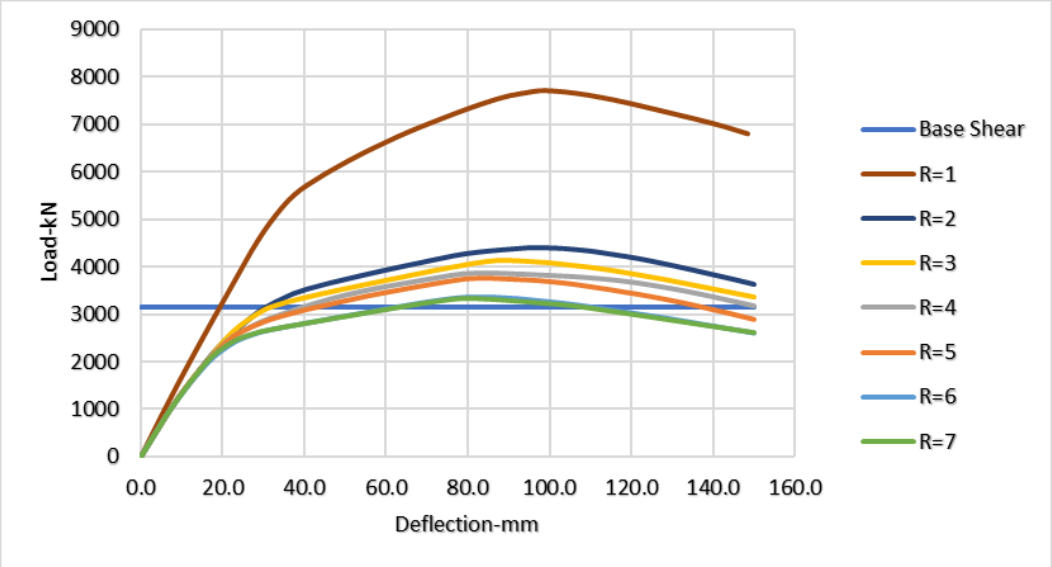

Figure 6.1: Capacity Curve of One Floor of The Frame Structure Building.

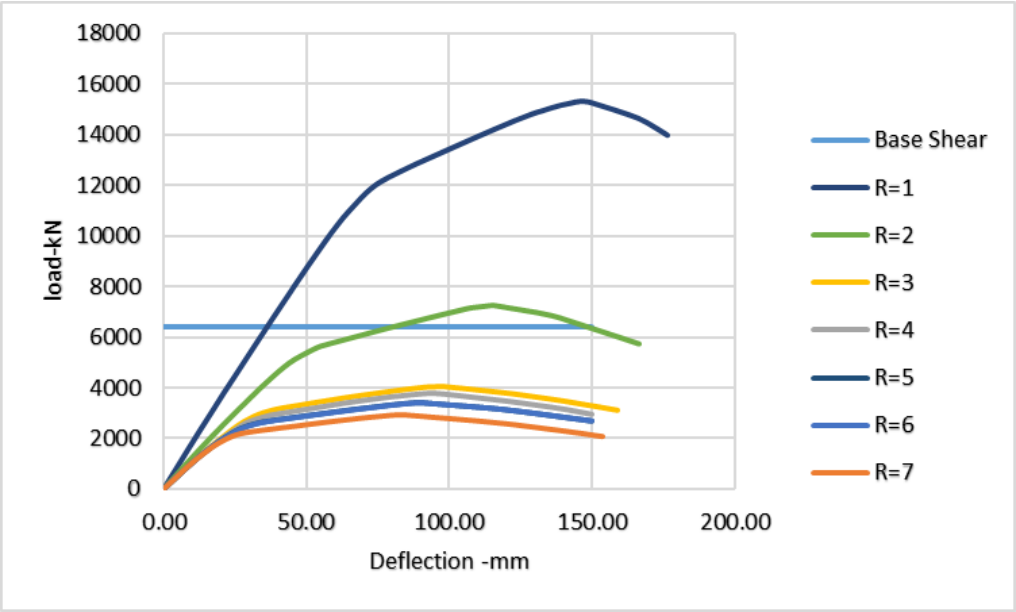

Figure 6.2: Capacity Curve of Two Floors of The Frame Structure Building.

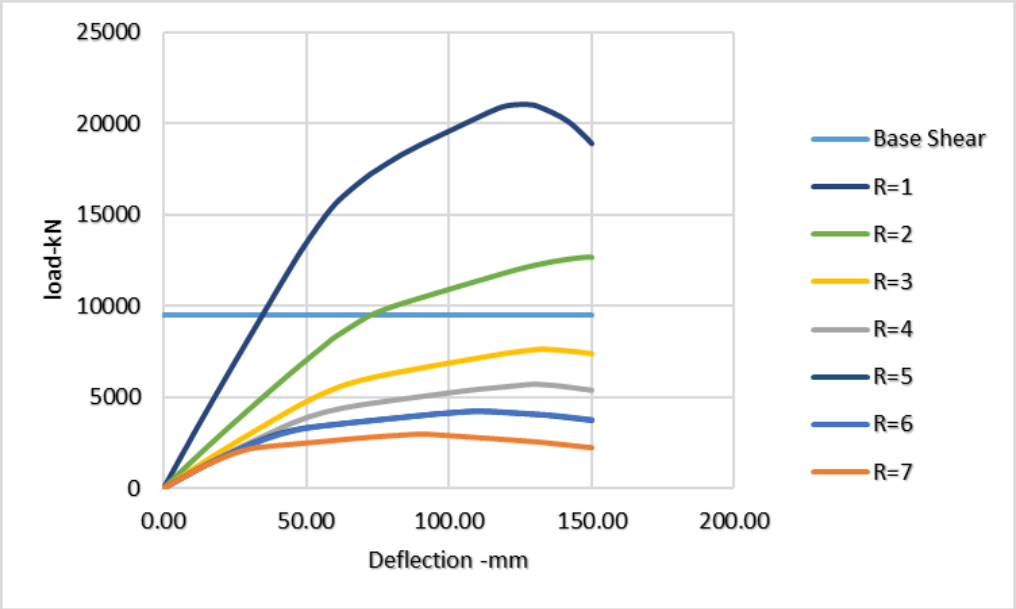

Figure 6.3: Capacity Curve of Three Floors of The Frame Structure Building.

Observing the results, it is evident that the building's ultimate behavior improves as the value of the response modification factor (R) decreases. Specifically, the behavior of the one-story building is similar when R is equal to 6 as compared to when R is equal to 7. The curves exhibit close alignment when R values range from 2 to 6. Conversely, a distinct change is noticed when R equals 1.

In the second Figure 6-2, showing a two-story building with doubled base shear, the ultimate behavior remains consistent for R values of 5 and 6. However, a significant change in the capacity curve is observed when R is equal to 2 and 1. This resembles the pattern seen in the three-story building, which exhibited a tripled base shear in the first case.

It can be seen the effect of number of stories on the behavior structure for one story building Figure 6.1 all forces are transmitted to the structure for all values of R. it can be seen also that all values are close to base except with R=1. For more than one story Figure 6.2 and 6.3 for R=1 and R=2 the seismic force is transmitted to the structure. Elastic behavior is observed for all buildings with different number of stories for R=1.

6.2 Effects of the redundancy factor

The second portion of results section will study the impact of the redundancy factor of the earthquake (ρ) on the behavior of the previous three floors frame building structure for each value of R from 1 to 7. The capacity curve (Load-Displacement Curve) is displayed in Figures (6-4) to (6-6). Here, the value of (ρ) is altered from 1.3 to 1, following the allowance granted by the ASCE-7-16 code under specific conditions outlined in code section 12.3.4. These conditions are applicable to the building studied in this research.

It is observed that the ultimate behavior of all curves diminishes when (ρ) is equal to 1. Notably, among the one-story building curves, the most fitting choice is the curve corresponding to R equaling 5, which aligns with the ASDCE value for an intermediate moment resisting frame. Furthermore, the base shear remains consistent across different values of (ρ).

The use of redundancy factor ρ = 1.3 is required for certain case. For seismic design category D, E and F the code requires to use ρ = 1.3. It can be seen that the ultimate load increases as expected with increasing the value of the redundancy factor.

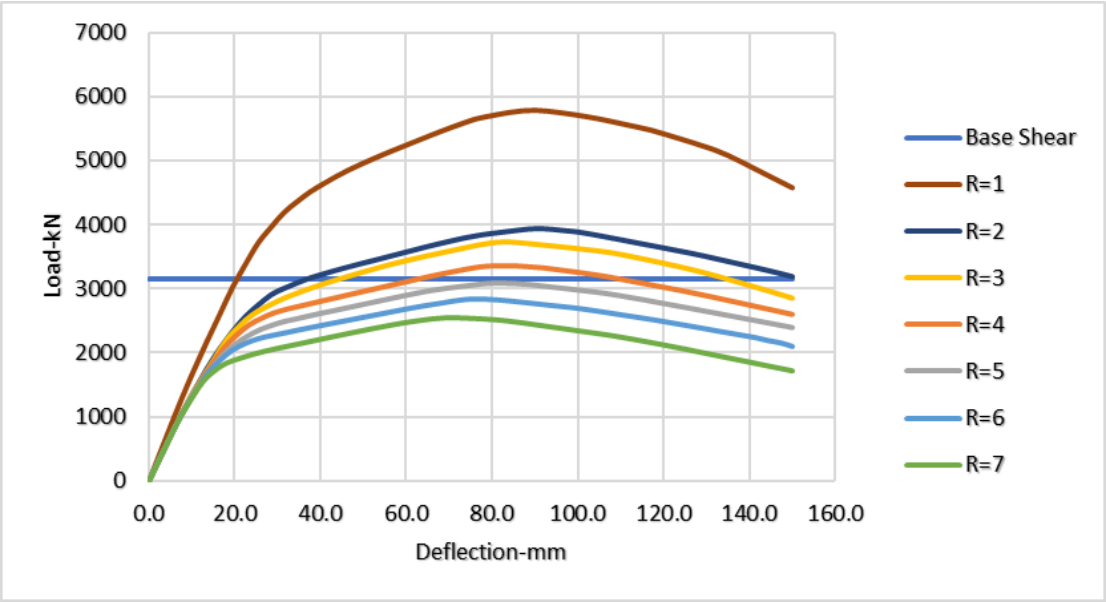

Figure 6.4: Capacity Curve of One Floor of The Frame Structure Building,

When ρ = 1.

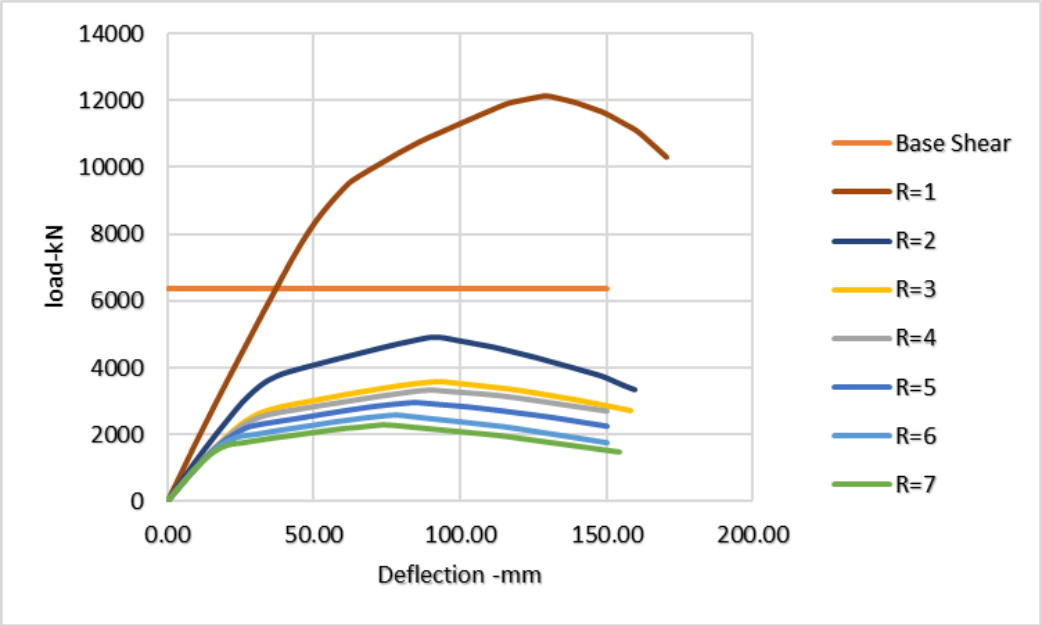

Figure 6.5: Capacity Curve of Two Floors of The Frame Structure Building,

When ρ = 1.

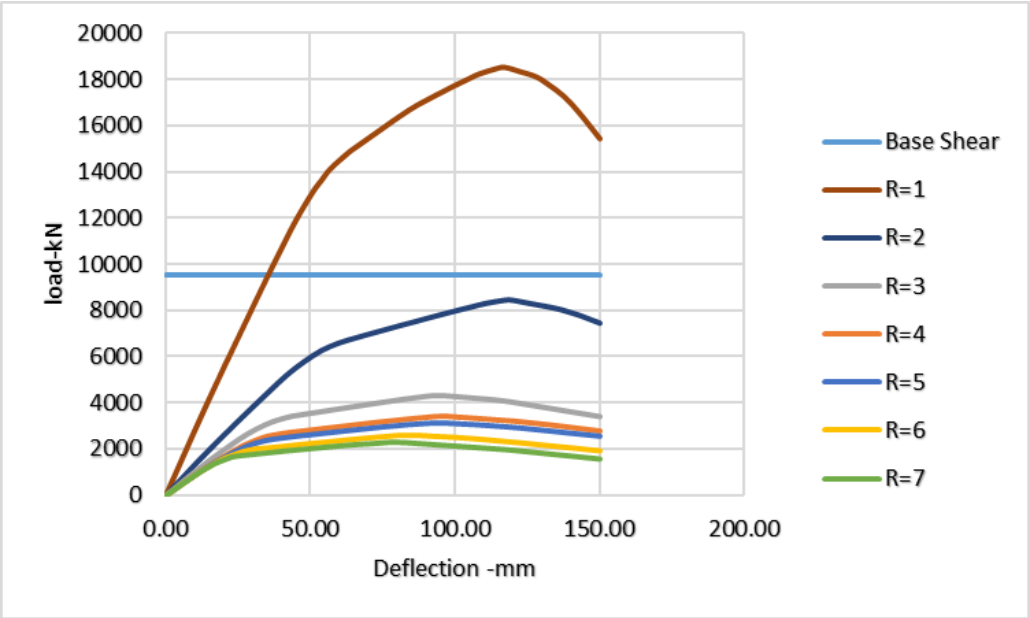

Figure 6.6: Capacity Curve of Three Floors of The Frame Structure Building,

When $\rho = 1$.

6.3 Effect of cross-sectional area

The third section of the analysis will present how changing the cross-sectional area and reinforcing ratio of reinforced concrete columns affect the behavior of a four-story intermediate moment resisting frame building (ground, first, second, and third floors) with the same characteristics as presented in Table 3-1. Throughout this section, the remaining parameters will remain consistent, including the ASCE 7-16 code-designated response modification factor (R = 5) and the redundancy factor (ρ = 1). Additionally, the importance factor is changed from (I = 1.25) to (I = 1). Various column sizes, measuring (55, 50, 45, 40, and 35) cm square is employed as shown in Figures ((6-7) – (6-10)), illustrating the capacity curves of the four-story intermediate moment resisting frame building (IMRF) structure with differing column cross-sectional areas.

It is worthy to note that the base shear values decrease from 3144 kN to 2516 kN for the one-story building, from 6382 kN to 5106 kN for the two-story building, and from 9522 kN to 7618 kN in the three-story building when the importance factor is reduced. Additionally, the ultimate behavior of frames with the same column cross-sectional area and the same response modification factor decreases. See Figure 5-10 for the case where R=5 and the column dimensions are 50x50 cm, and Figure 5-13 for the case involving COL 50x50 cm. This observation holds true across all curves.

.

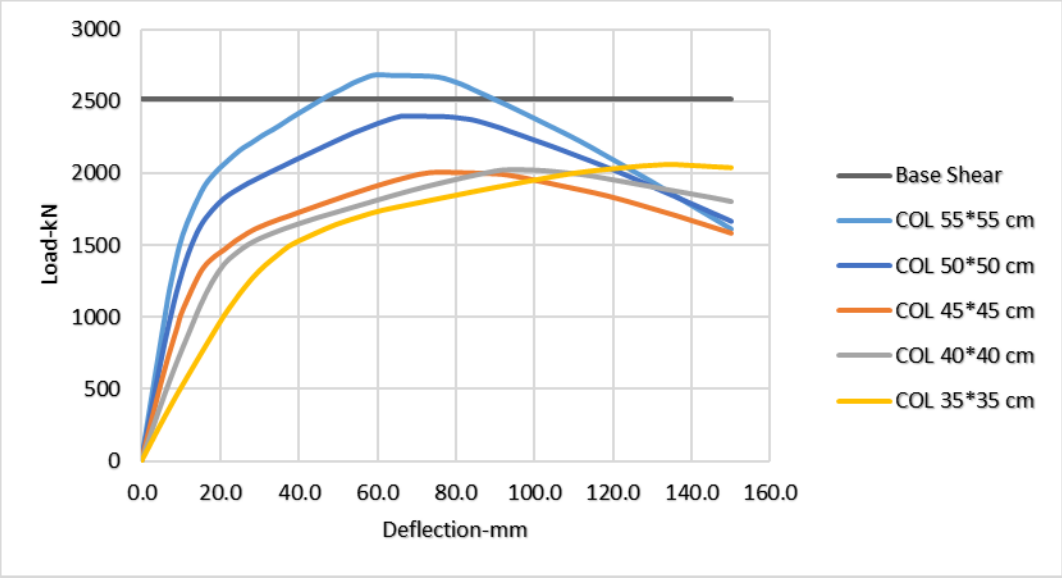

Figure 6.7: Capacity Curve of One Floor of The Frame Structure Building,

With Different Cross Sectional Area of Columns.

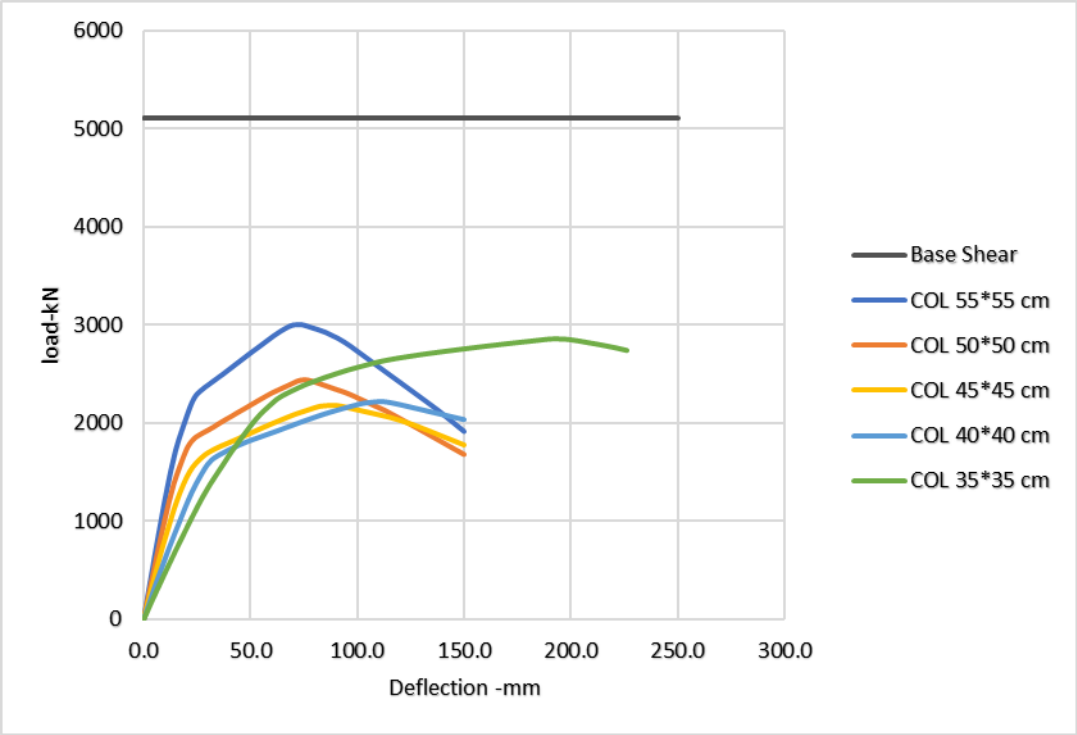

Figure 6.8: Capacity Curve of Two Floors of The Frame Structure Building,

With Different Cross Sectional Area of Columns.

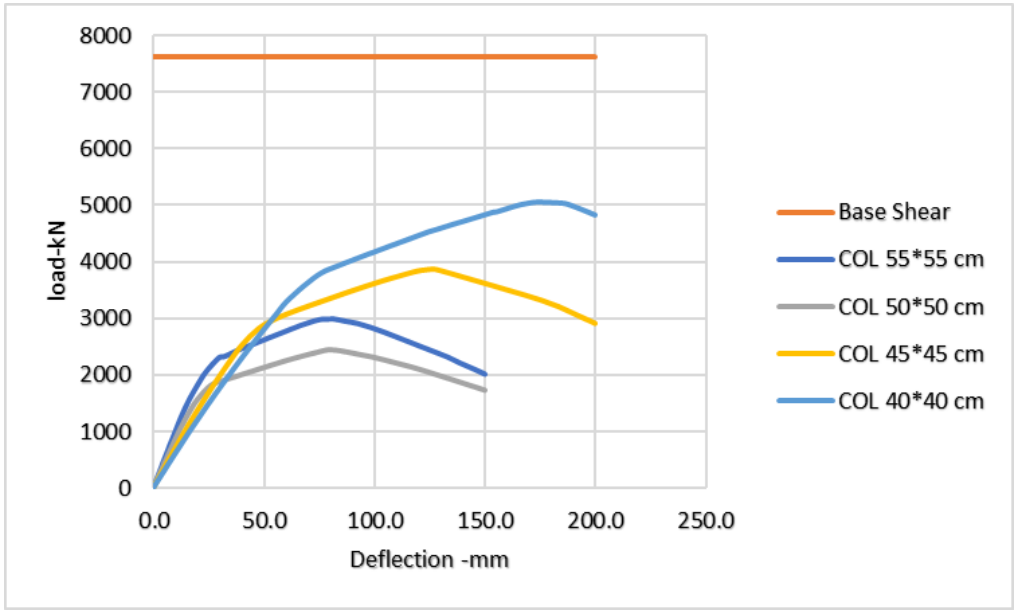

Figure 6.9: Capacity Curve of Three Floors of The Frame Structure Building, With Different Cross Section Area of Columns.

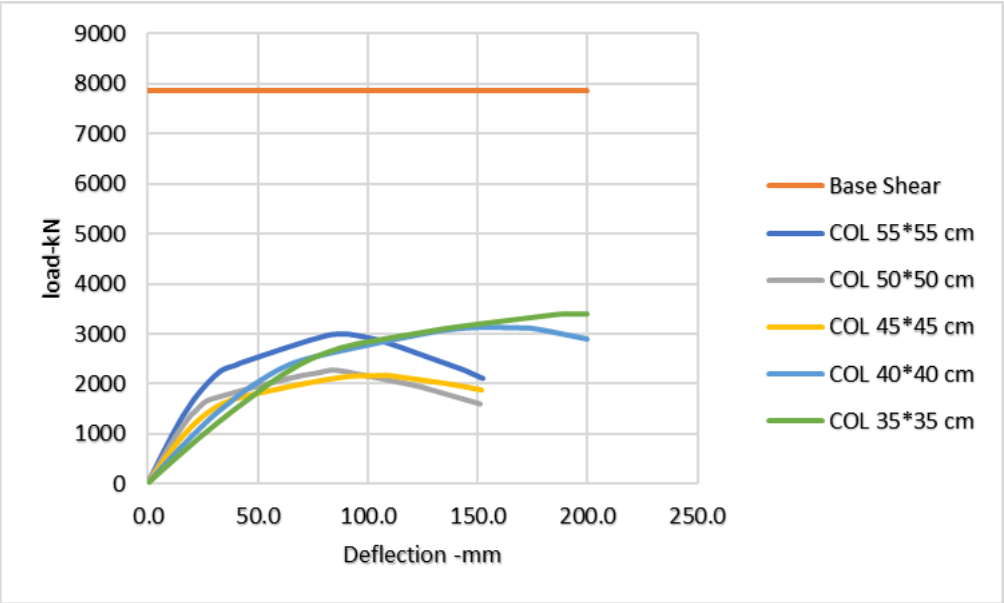

Figure 6.10: Capacity Curve of Four Floors of The Frame Structure Building, With Different Cross Section Area of Columns.

Figures ((6.7) -(6.10)) shows the effect of the cross section on the behavior of the building which in turn effect the value of R. This means that different value of R could be obtained for different value of cross sections dimensions.

6.4 Effects of reinforcement ratio.

According to the previous capacity curve of the four-frame building depicted in Figures ((6-7)- (6-10)), and by applying Equation (30-33), the actual value of the response modification factor (R) was computed to validate the original design selection based on the ASCE 7-16 code, which was set at 5. The obtained results reveal that the true value of R matches with the code-specified value only on the Ground Floor, within a range of column reinforcement ratios between (1.26-1.5) %. This consistency occurs in the case of a one-story building. However, as the number of floors increases, this alignment diminishes, reaching a value of (R=3.3) with a minimum reinforcement ratio of 1.01% for a three-story building, as indicated in Table 6-1. This table shows the manually calculated actual values of R alongside the maximum lateral displacement (Performance Point) in each respective case.

Table 6.1: Actual Value of R and Performance Point for Each Story and Cross-Sectional Area.

Number of Stories	section (cm)	du max (mm)	dy (mm)	M	R	PP (mm)	% Reinf. Ratio
One Story	55*55	60.5	7.5	8.1	3.9	20	1.04
	50*50	68.5	6	11.4	4.7	22	1.02-1.22
	45*45	76.5	6	12.8	4.9	25	1.26-1.51
	40*40	94.5	9	10.5	4.5	29	1.59-2.36
	35*35	133.5	12	11.1	4.6	36	1.81-4.01
Two Stories	55*55	73.1	10.5	7.0	3.6	30	1.01
	50*50	75.4	9.7	7.8	3.8	33	1.02-1.22
	45*45	85.9	9.7	8.9	4.1	38	1.26-1.51
	40*40	109.3	10.5	10.4	4.5	43	1.59-2.45
	35*35	195.1	25	7.8	3.8	52	4.62-5.25
Three Stories	55*55	81.8	13.5	6.1	3.3	41	1.01
	50*50	80.6	12	6.7	3.5	46	1.02-1.22
	45*45	126.6	16	7.9	3.9	50	2.42-3.18
	40*40	176.3	16	11.0	4.6	47	4.71-6.03
Four Stories	55*55	90.1	14.5	6.2	3.4	52	1.01
	50*50	85.2	12.8	6.7	3.5	60	1.02
	45*45	107.3	11.1	9.7	4.3	65	1.01-2.42
	40*40	155.5	14	11.1	4.6	70	2.36-5.03
	35*35	198.6	24	8.3	3.9	78	4.81-6.03

Therefore, the proposed values of the response modification factor in Table 6-1 are approximately 4. Subsequently, the design and manual calculations were re- designed and re-calculated using a different R-value of 4. The aim was to bridge the gap between the analysis and designed response modification factor values, aiming for an appropriate value within the context of multi-story intermediate moment resisting frame buildings, as employed in this research. The capacity curves for the multi-story structural building are re-presented to include only some of the previously mentioned column cross-sectional areas, which exhibited reasonable reinforcement ratios. Therefore, cross-sectional areas of (35 and 55) cm were excluded from Figures ((6-11) -(6-14)), with their corresponding manual calculations presented in Table 6-2 as indicated below.

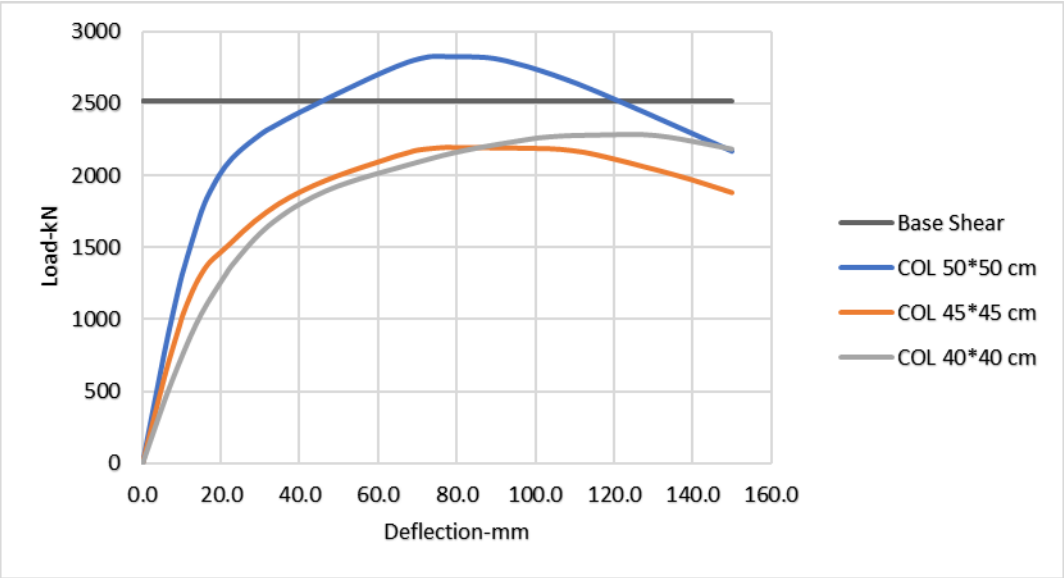

Figure 6.11: Capacity Curve of One Floor of The Frame Structure Building, With Different Cross Section Area of Columns.

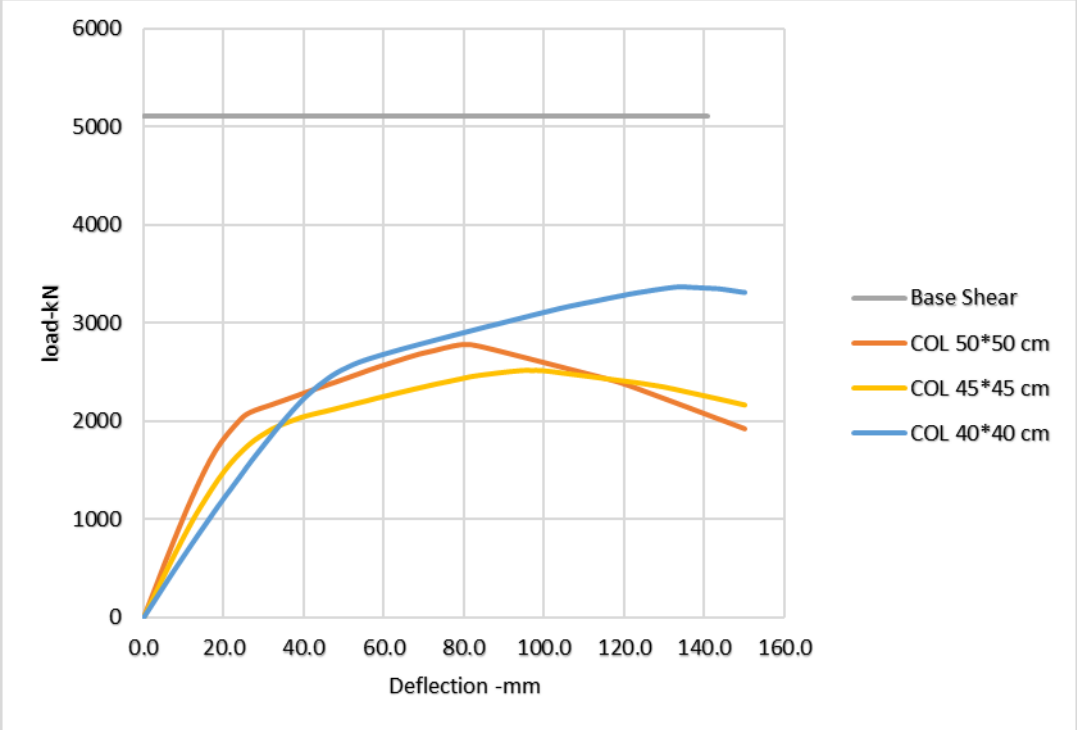

Figure 6.12: Capacity Curve of Two Floors of The Frame Structure Building, With Different Cross Section Area of Columns.

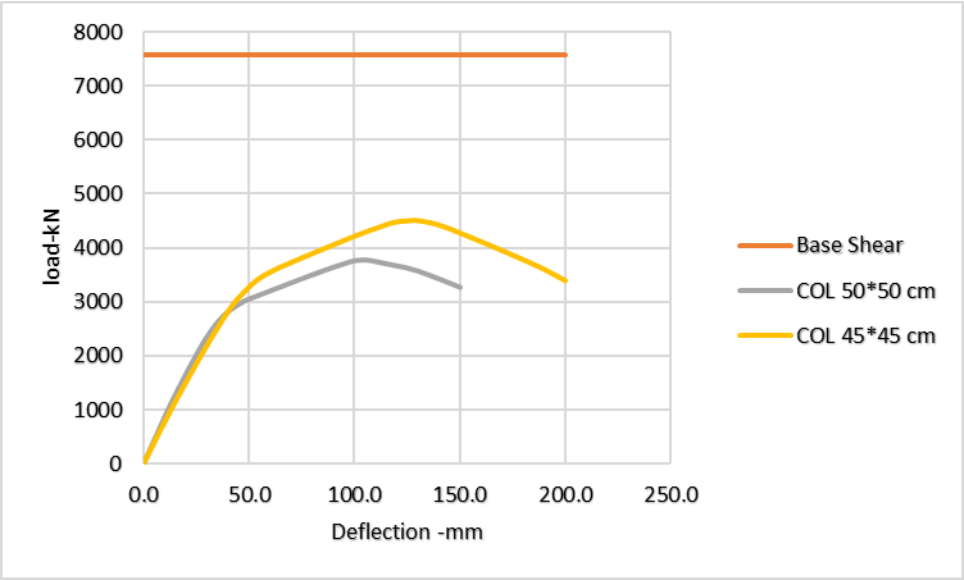

Figure 6.13: Capacity Curve of Three Floors of The Frame Structure Building, With Different Cross Section Area of Columns.

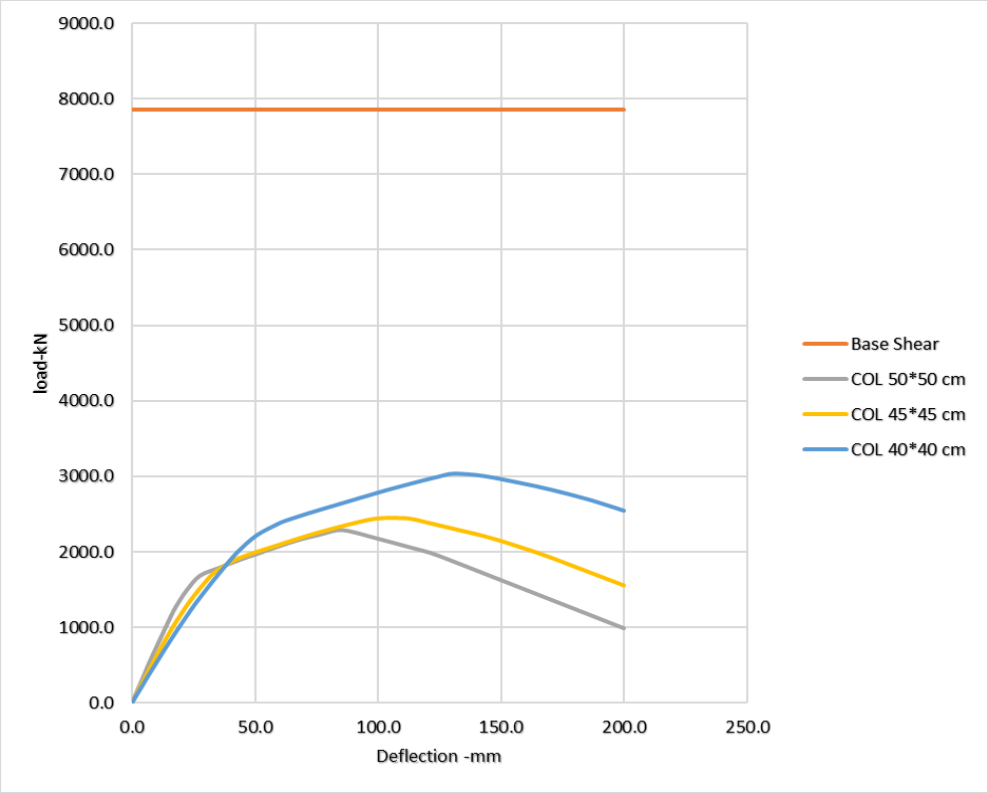

Figure 6.14: Capacity Curve of Four Floors of The Frame Structure Building, With Different Cross Section Area of Columns.

Table 6.2: Actual Value of R and Performance Point for Each Story and Cross-Sectional Area.

Number of Stories	section (cm)	du max (mm)	dy (mm)	M	R	PP (mm)	% Reinf. Ratio
One Story	50*50	74.7	9	8.3	3.9	22	1.22-1.82
	45*45	79.4	9	8.8	4.1	25	1.51-1.86
	40*40	124.5	15	8.3	3.9	30	1.26-2.85
Two Stories	50*50	80.6	9	9	4.1	33	1.26
	45*45	96.9	10.5	9.2	4.2	38	1.26-1.86
	40*40	134.9	15	9	4.1	45	2.36-3.85
Three Stories	50*50	103.9	12	8.7	4	44	1.82
	45*45	129.3	16	8.1	3.9	48	1.88-3.04
Four Stories	50*50	85.2	11.95	7.1	3.6	60	1.02
	45*45	104.6	13	8	3.9	62	1.26-2.42
	40*40	132.6	16	8.3	3.9	65	2.36-3.04

6.5 performance level of the IMRF

The last section of the analysis results will display the performance levels in response to earthquakes, categorized as Immediate Occupancy (IO), Life Safety (LS), and Collapse Prevention (CP). It will also examine the correlation between these performance levels and the number of steps taken. Table 5-10 provides the number of steps required to achieve each of the three aforementioned performance levels. Meanwhile, Figures (6-15) to (6-24) display the performance level reached by the frame building structure at the performance point for each case as demonstrated in Table 6-3.

Table 6.3: Step Number and Performance Levels for Four Stories Frame Structural Building.

Number of Stories	Col Dimension (cm)	Step Number	Performance Level
One Story	COL 50*50	6	IO
		8	LS
		11	CP
	COL 45*45	6	IO
		8	LS
		12	CP
	COL 40*40	6	IO
		8	LS
		13	CP
Two Stories	COL 50*50	6	IO
		7	LS
		10	CP
	COL 45*45	6	IO
		7	LS
		10	CP
	COL 40*40	11	IO
		12	LS
		18	CP
Three Stories	COL 50*50	9	IO
		10	LS
		16	CP
	COL 45*45	8	IO
		9	LS
		13	CP
Four Stories	COL 50*50	6	IO
		7	LS
		10	CP
	COL 45*45	6	IO
		8	LS
		11	CP
	COL 40*40	8	IO
		9	LS
		11	CP

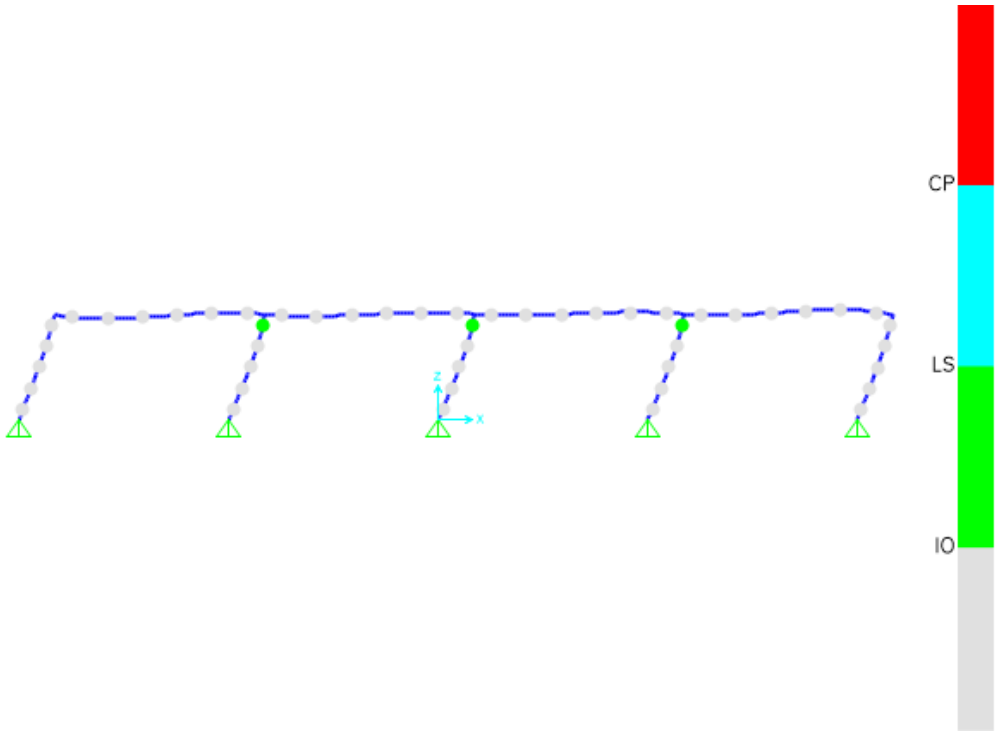

Figure 6.15: The Performance Level at The Performance Point for One-Story Building, When Col 50*50 cm.

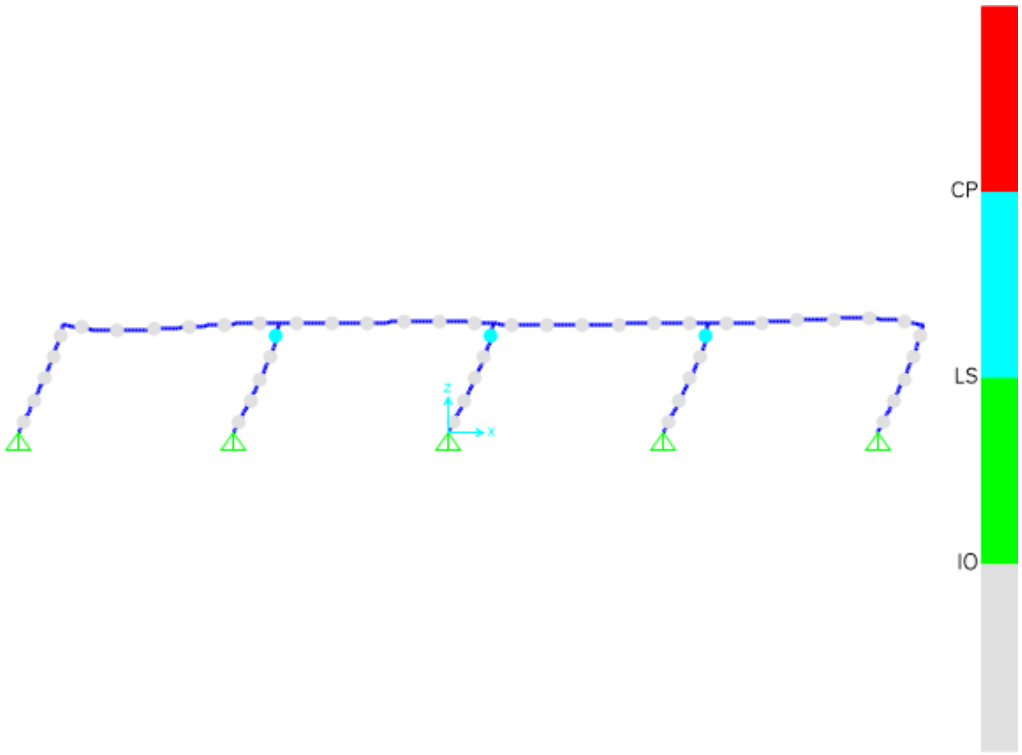

Figure 6.16: The Performance Level at The Performance Point for One-Story Building, When Col 45*45 cm.

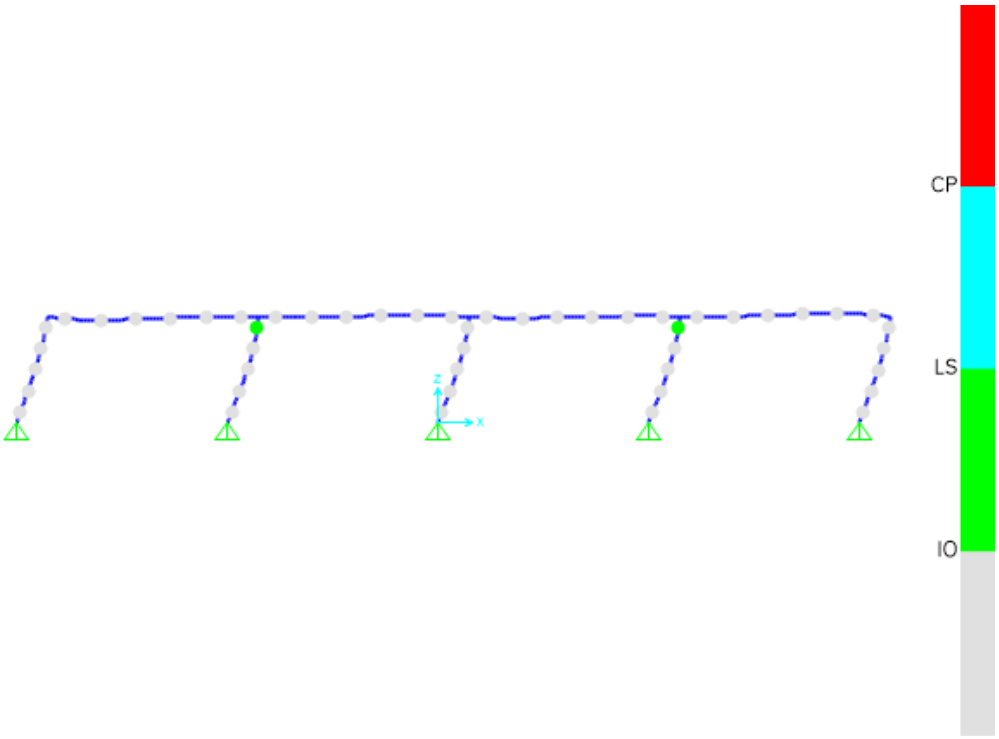

Figure 6.17: The Performance Level at The Performance Point for One-Story Building, When Col 40*40 cm.

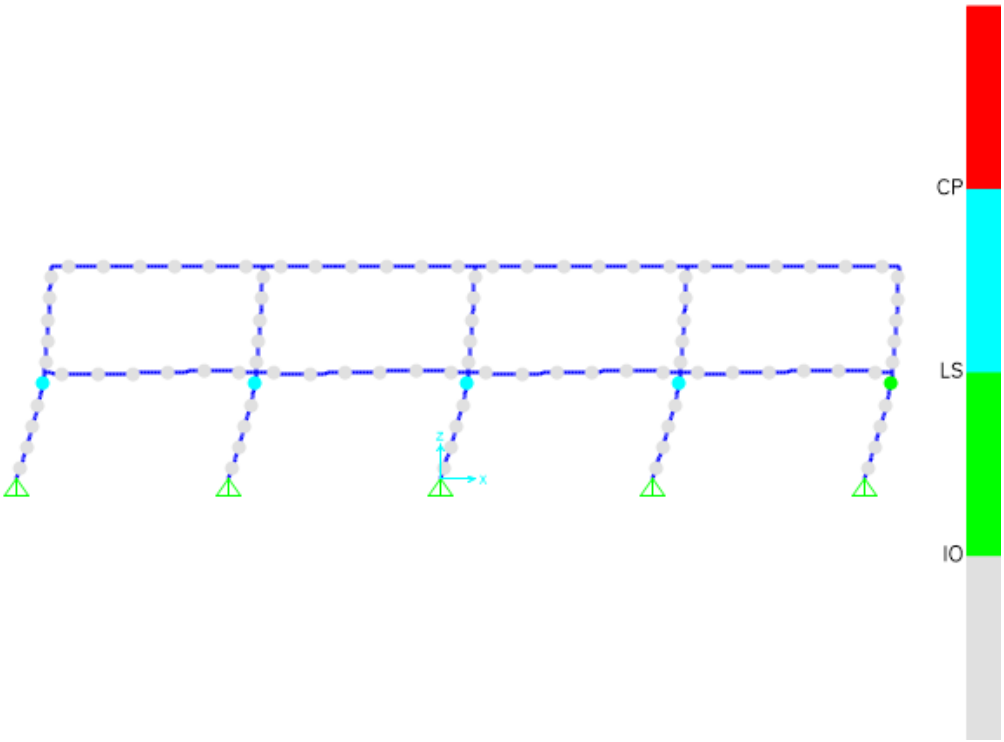

Figure 6.18: The Performance Level at The Performance Point for Two-Story Building, When Col 50*50 cm.

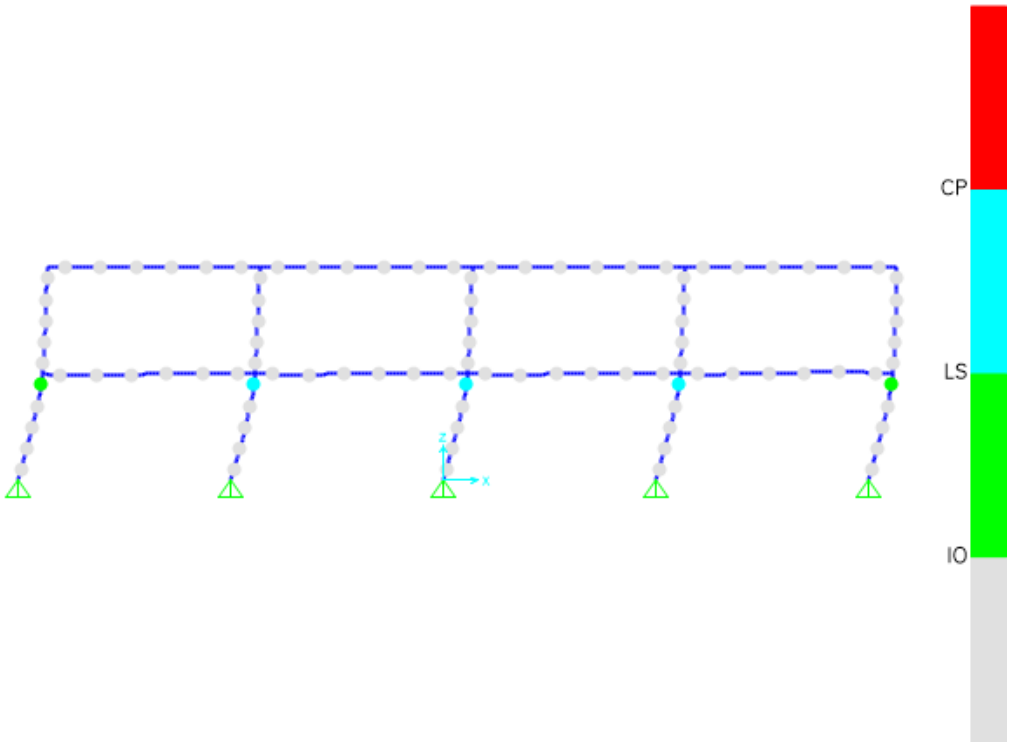

Figure 6.19: The Performance Level at The Performance Point for Two-Story Building, When Col 45*45 cm.

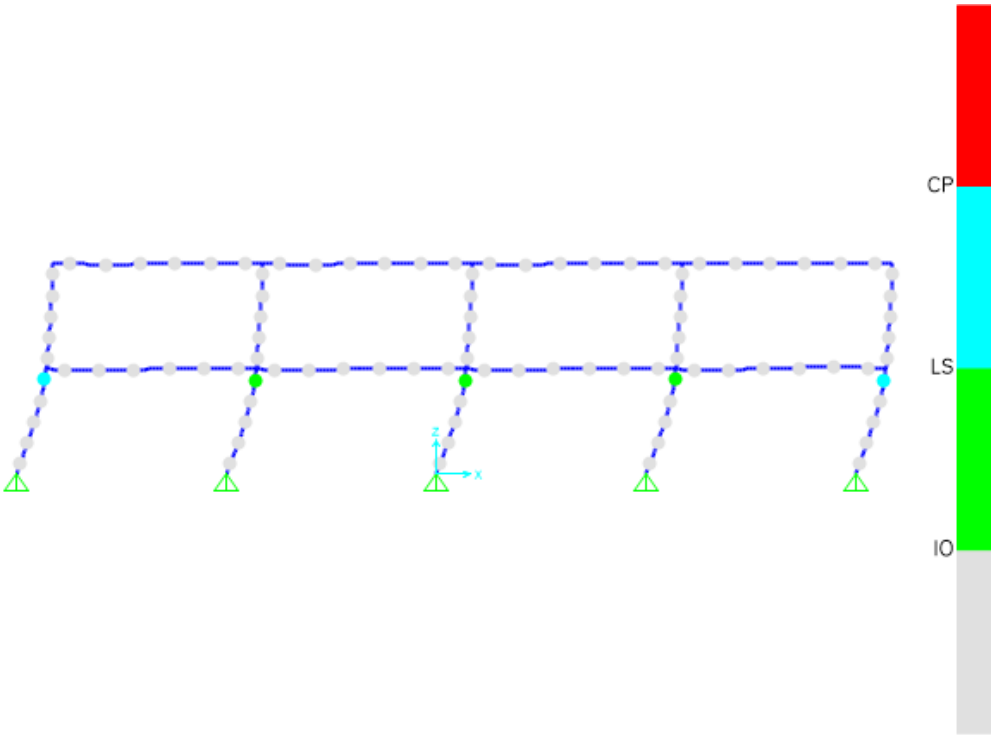

Figure 6.20: The Performance Level at The Performance Point for Two-Story Building, When Col 40*40 cm.

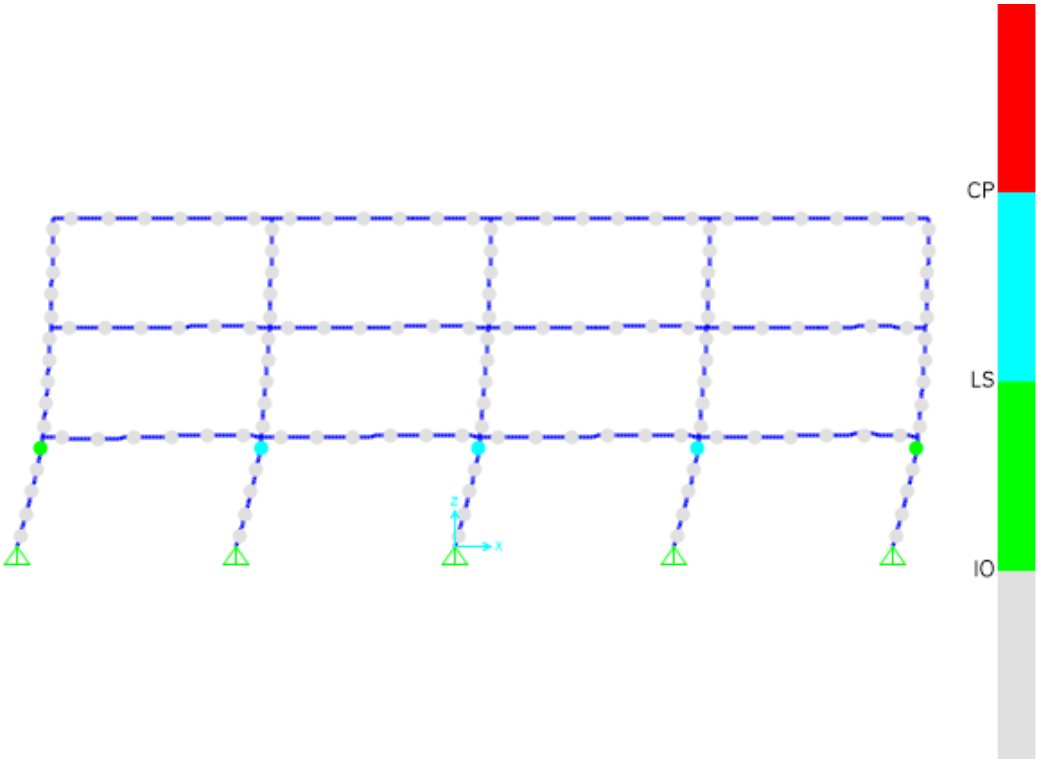

Figure 6.21: The Performance Level at The Performance Point for Three-Story Building, When Col 50*50 cm.

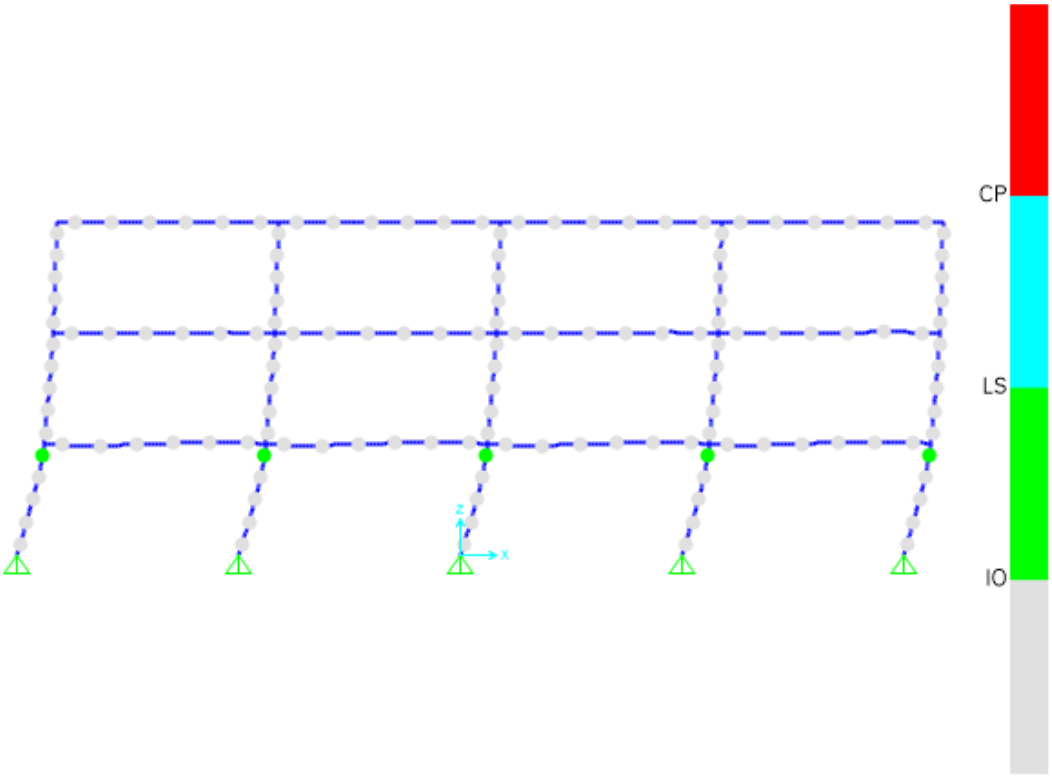

Figure 6.22: The Performance Level at The Performance Point for Three-Story Building, When Col 45*45 cm.

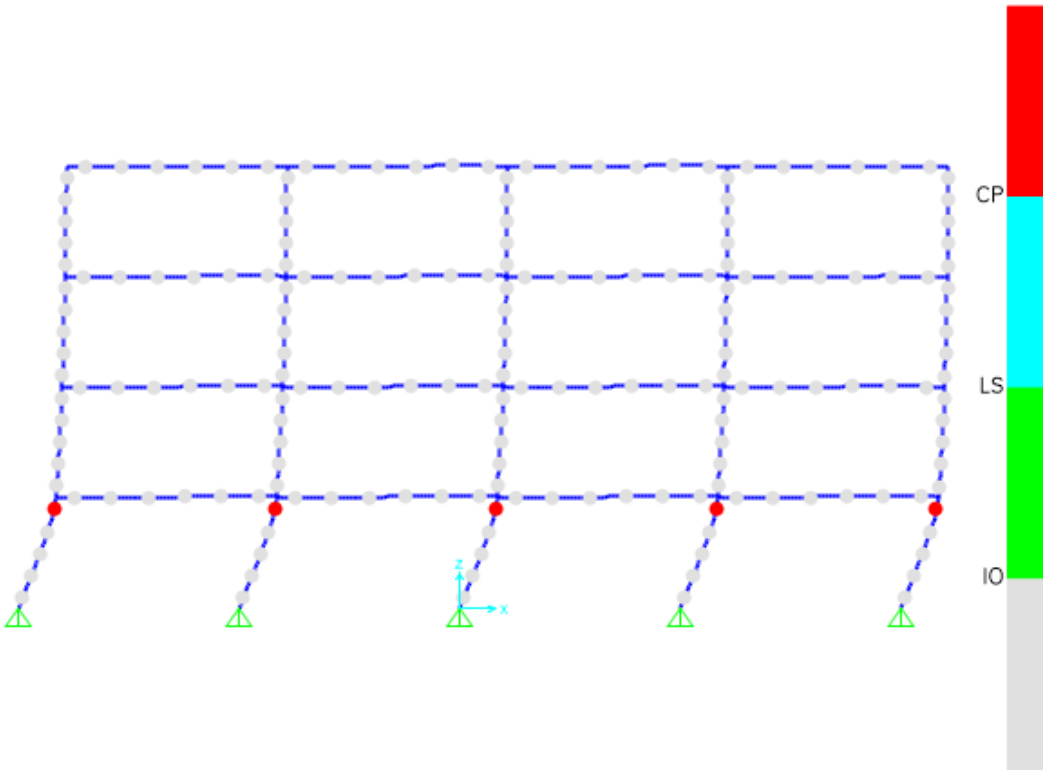

Figure 6.23: The Performance Level at The Performance Point for Four-Story Building, When Col 50*50 cm.

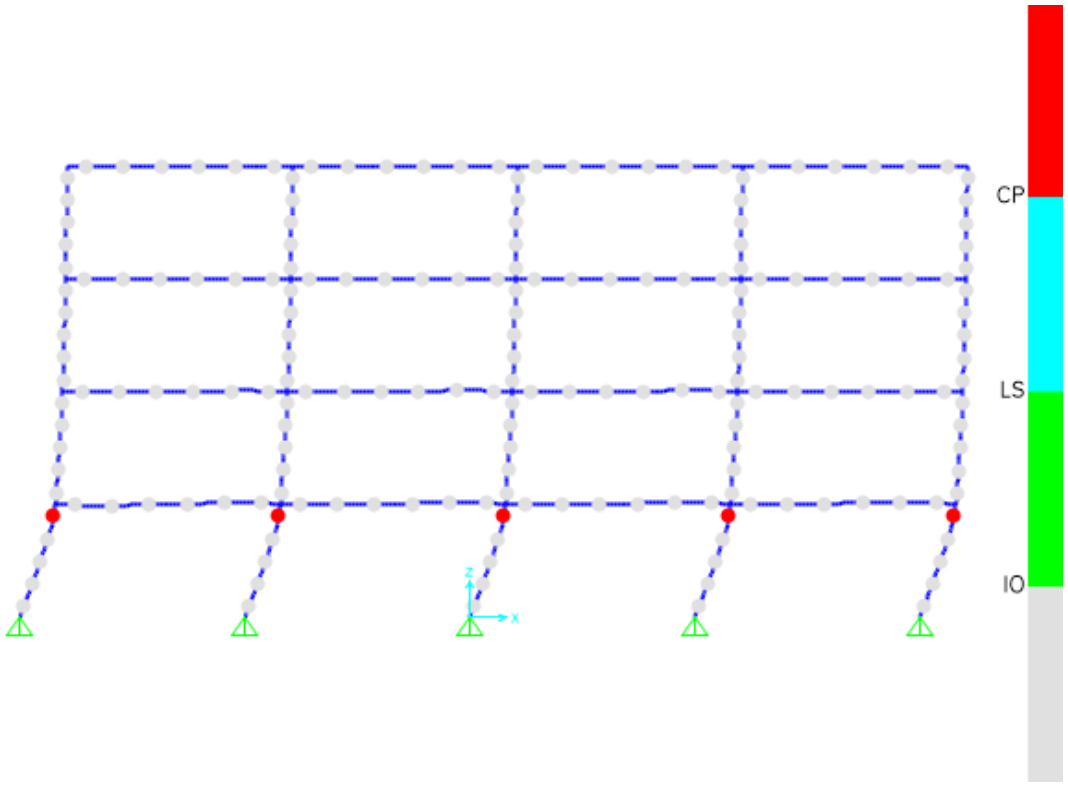

Figure 6.24: The Performance Level at The Performance Point for Four -Story Building, When Col 45*45 cm.

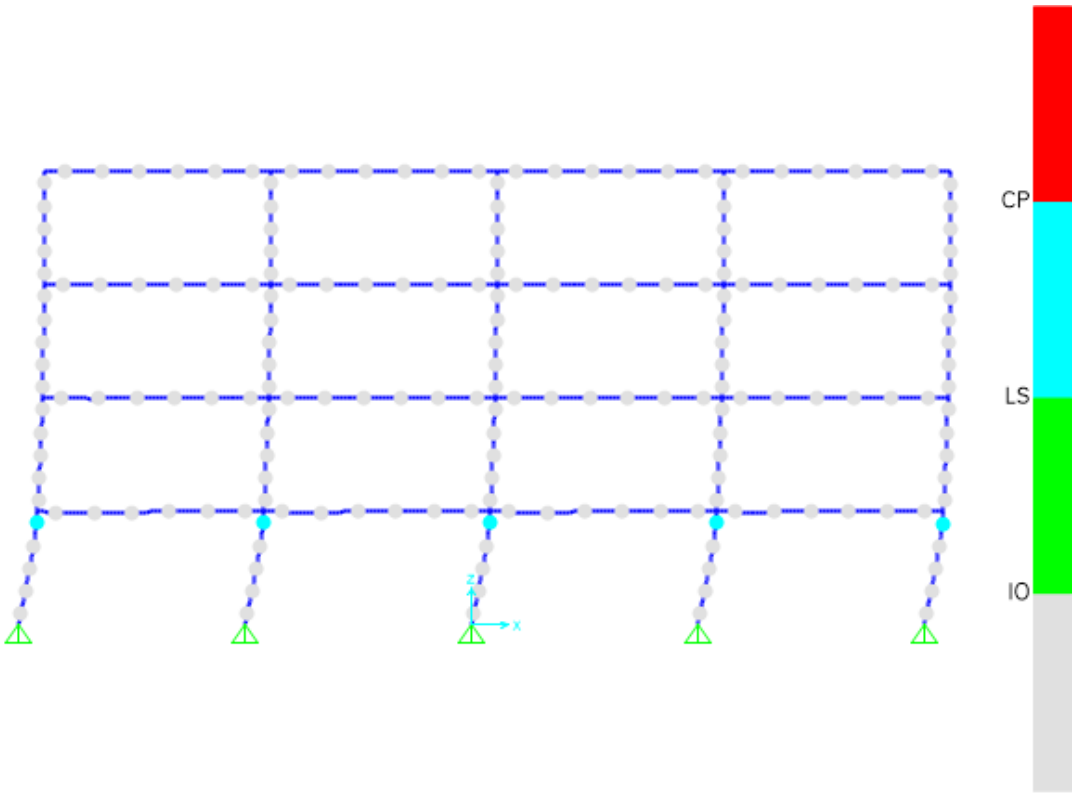

Figure 6.25: The Performance Level at The Performance Point for Four-Story Building, When Col 40*40 cm.

CHAPTER 7:CONCLUSIONS AND FUTURE WORK

7.1 Conclusions

The main purpose of this research is to estimate and evaluate the response modification factor (also known as R-factor) of an intermediate moment-resisting RC-frame. To achieve this research goal, a series of 3D-frame structures of 1, 2, 3, and 4 stories with response modification factors ranging from 1 to 7, and with columns of dimensions (55, 50, 45, 40, and 35) cm^2, are designed. These designs vary in reinforcement ratios and are developed following the guidelines of the ACI-318 (18.4) code.

A nonlinear static pushover analysis is performed on each frame structure to determine the R-factor. The pushover analysis takes into account both gravity loads and p-delta effects. Subsequently, the capacity curve of each frame structure (i.e., the result of pushover analysis) is exhibited.

Using the procedure explained in this study, the R-factor and the displacement ductility ratio (μ) for each frame construction are computed. The following conclusions are the main findings of this research study:

1. The ultimate behavior of the intermediate moment resisting frame is affected by the response modification factor value is used which in turn is slightly influenced by the number of stories in a positive relationship. While being affected by an inverse relationship with the redundancy and importance factors.

2. The R-factor value has a significant impact on the design, and the behavior varies significantly according to the design, particularly in relation to vertical elements like columns. As a result, this variation can differ from one designer to another, which in turn affects the analysis.

3. The ASCE code value used for the intermediate moment resisting frame for a multi-story building (R=5) gives response modification factor R=4 when it obtained using numerical analysis. The proposed R for the intermediate moment frame is 4. Since the analysis and design value gives the same value.

4. It was discovered that with a reinforcement ratio of approximately 2.42% and a column cross-sectional area of (45*45) cm, the highest value of the ductility factor is achieved. As a result, this configuration provides the optimal arrangement for the response modification factor (R).

5. We conclude that the fiber hinges pushover analysis method, employing nonlinear analysis through the SAP2000 software, proves to be an efficient approach, yielding satisfactory and rapid results in comparison to alternative software and methods.

7.2 Future Work

1. A diaphragm investigation of the reinforced concrete moment resisting frames should be conducted in future research to study its influence on the ultimate behavior, maximum lateral displacement, and its correlation with the response and overstrength modification factors.

2. The model could be analyzed for a greater number of stories, exceeding four, to examine the effect of using different number of bays in each direction.

3. To conduct a time history analysis of the reinforced concrete moment resisting frames and compare its results with those of the nonlinear pushover analysis.

4. To investigate the real behavior and determine an appropriate value for the response modification factor in multistory buildings in comparison to other types of frames, including both ordinary and special moment-resisting frames.

5. To attempt to minimize the column sections as the number of floors increases, particularly in tall buildings exceeding five stories.

6. Different software could be used and different method to overcome the stiffened shape of load curve.

REFERENCES

- Abdi H, Hejazi F, Jaafar MS, Abd Karim IB. Response modification factors for reinforced concrete structures equipped with viscous damper devices. Periodica Polytechnica Civil Engineering. 2018;62(1):11-25.
- Abdi H, Hejazi F, Jaafar MS. Response modification factor-Review paper. InIOP Conference Series: Earth and Environmental Science 2019 Nov 1 (Vol. 357, No. 1, p. 012003). IOP Publishing.
- Abou-Elfath, H., & Elhout, E. (2018). Evaluating the response modification factors of RC frames designed with different geometric configurations. *International Journal of Civil Engineering, 16,* 1699–1711.
- ACI (American Concrete Institute). Building code requirements for structural concrete and commentary. ACI 318-08. American Concrete Institute, Farmington Hills, Michigan, USA; 2008.
- A. S. Elnashai and A. M. Mwafy, "Overstrength and force reduction factors of multistory reinforced-concrete buildings," *The Structural Design of Tall Buildings*, vol. 11, no. 5, pp. 329-351, 2002
- Aliakbari, F., & Shariatmadar, H. (2019). Seismic response modification factor for steel slit panel-frames. *Engineering Structures, 181,* 427–436.
- American Concrete Institute. Building code requirements for reinforced concrete, ACI 318-95, 99, 02, Detroit, Michigan, 1995, 1999, 2002.
- American Society of Civil Engineers, "*Minimum Design Loads and Associated Criteria for Buildings and Other Structures, ASCE/SEI 7-16*. Reston, Virginia, 2016.
- Applied Technology Council (ATC), Structural Response Modification Factors (ATC-19), Redwood City, California, 1995.
- Asgarian B, Shokrgozar HR. BRBF response modification factor. Journal of constructional steel research. 2009 Feb 1;65(2):290-8.
- Asghari, A., & Zarnagh, B. A. (2017). A new study of seismic behavior of perforated coupled shear walls. *International Journal of Civil Engineering, 15,* 775–789.
- ATC, 1982b, An Investigation of the Correlation Between Earthquake Ground Motion and Building Performance, ATC-10 Report, Applied Technology Council, Redwood City, California.

- ATC. Tentative provisions for the development of seismic regulations for buildings. ATC-3-06, Applied Technology Council, Redwood City, California, 1978:45–53.
- ATC. (1995), A critical review of current approaches to earthquake resistant design. ATC-34,"Applied Technology Council", Redwood City, California, 1995:31–6
- B. BRESLER and A. C. SCORDELIS, Shear strength of reinforced concrete beams, ACI- Journal, Proceedings, Vol.60 No.1, Jan. (1963), PP.3 7-51
- Badal, P. S., & Sinha, R. (2019). Assessment of response reduction factor for reinforced concrete frame buildings in a probabilistic seismic risk framework. *Recent Advances in Structural Engineering, 2*, 255–267.
- Bathe K. Finite element procedures. Englewood Cliffs, NJ: Prentice-Hall; 1996.
- Bresler B, Scordelis AC. Shear strength of reinforced concrete beams. In Journal Proceedings 1963 Jan 1 (Vol. 60, No. 1, pp. 51-74).
- Chen, X. L., Fu, J. P., Xue, F., & Wang, X. F. (2017). Comparative numerical research on the seismic behavior of RC frames using normal and high-strength reinforcement. *International Journal of Civil Engineering, 15,* 531–547.
- C. M. Uang, "Establishing R (or Rw) and Cd factors for building seismic provisions," Journal of Structural Engineering, vol. 117, no. 1, pp. 19-28, 1991.
- Dal Lago B, Molina FJ. Assessment of a capacity spectrum seismic design approach against cyclic and seismic experiments on full scale precast RC structures. Earthquake engineering & structural dynamics. 2018 Jun;47(7):1591-609.
- Daza L. G. Correlation between minimum building strength and the response modification factor. Taylor & Francis Group, London, 2010.
- D. Ugalde and D. Lopez-Garcia, "Behavior of reinforced concrete shear wall buildings subjected tolarge earthquakes," Procedia Engineering, vol. 199, no., pp. 3582-3587, 2017.
- Eberhard MO, Meigs BE. Earthquake-resisting system selection statistics for reinforced concrete buildings. Earthquake spectra. 1995 Feb;11(1):19-36.
- Fanaie N, Dizaj EA. Response modification factor of the frames braced with reduced yielding segment BRB. Structural Engineering and Mechanics. 2014 Apr 10;50(1):1-7.
- Fast P, Gafner B, Jackson R. Eighteen story hybrid mass timber student residence at the University of British Columbia. Structural Engineering International. 2017 Feb 1;27(1):44-8.
- Freeman, S.A. (1990). "On the Correlation of Code Forces to Earthquake Demands." Applied Technology Council, Redwood City, California.

- G. MUELLER, Numerical problems in nonlinear analysis of reinforced concrete Report No. UC SESM 77-5, Department of Civil concrete, Report No. UC SESM 77-5, Department of Civil Engineering University of California, Berkeley, Sept. 1977.
- Galasso, C., Maddaloni, G.and Cosenza, E. (2014). "Uncertainly Analysis of Flexural Overstrength for Capacity Design of RC Beams." DOI: 10.1061/(ASCE)ST.1943-541X.0001024.
- H. DUDDECK, G. GRIEBEN OW, and G. SCHAPER 'Auszuge aus dem sechsten arbeitsbericht z um forschungsvorhaben stahlbetonplatten mit nichtline aren stoffgesetzen', Arbeitsbericht Braunschweig, 1976.
- Han SW, Jee NY. Seismic behaviors of columns in ordinary and intermediate moment resisting concrete frames. Engineering structures. 2005 May 1;27(6):951-62.
- Hanson, R. D., Aiken, I. D., Nims, D. K., Richter, P. J., and Bachman, R. E. (1993). ''State-of-the art and state-of-the-practice in seismic energy dissipation.'' Proc., Seminar on Seismic Isolation, Passive Energy Dissipation, and Active Control, ATC-17-1 Rep. No. 449–471, Applied Technology Council, Redwood City, Calif.
- Hejazi, F., Kojouri, S. J., Noorzaei, J., Jaafar, M. S., Thanoon, W. A., Abang Abdullah, A. A. "Inelastic seismic response of RC building with control system.". *Key Engineering Materials,* Vol. 462–463, pp 241–246.
- Hejazi, F., Toloue, I., Jaafar, M.S. "Optimization of earthquake energy dissipation system by genetic algorithm.". *Computer-Aided Civil and Infrastructure Engineering,* 28(10), pp. 796–810. 2013.
- Hognestad, E. "A study on combined bending and axial load in reinforced concrete members." Univ. of Illinois Engineering Experiment Station, Univ. of Illinois at Urbana-Champaign, IL, 43-46, (1951).
- Hu W, Thomson PF. An evaluation of a large time increment method. Comput Struct 1996;58(3):633–8.
- Hu YX, Liu SC, Dong W. Earthquake engineering. CRC Press; 1996 Jul 18.
- Izadinia M, Mohammad Ali Rahgozar, Omid Mohammadrezaei. (2012)." Response modification factor for steel moment-resisting frames by different pushover analysis methods." Journal of Constructional Steel Research 79 (2012) 83–90.
- Izadinia, M., Rahgozar, M. A., & Mohammadrezaei, O. (2012). Response modification factor for steel moment-resisting frames by different pushover analysis methods. *Journal of Constructional Steel Research, 79,* 83–90.

- Jianzhuang Xiao, Yuedong Sun, H. Falkner, Seismic performance of frame structures with recycled aggregate concrete, Eng. Struct. 28 (2006).
- Kaljevic I, Patnaik SN, Hopkins DA. Development of finite elements for two-dimensional structural analysis using the integrated force method. Comput Struct 1996;59(4):691–706.
- Kappos AJ, Paraskeva TS, Moschonas IF. Response modification factors for concrete bridges in Europe. Journal of Bridge Engineering. 2013 Dec 1;18(12):1328-35.
- Kappos, A.J. (1999). “Evaluation of Behavior Factors on the Basis of Ductility and Overstrength Studies.” Engineering Structures, 21, 823–835, 1999.
- Kent, D.C., and Park, R. "Flexural members with confined concrete." Journal of the Structural Division, Proc. of the American Society of Civil Engineers, 97(ST7), 1969-1990, (1971).
- Khy K, Chintanapakdee C. Quantification of Different Sources of Over-Strength in Seismic Design of a Reinforced Concrete Tall Building. Engineering Journal. 2019 Nov 30;23(6):209 23.
- Kim J, Choi H. (2005). “Response modification factors of chevron-braced frames. Journal of Engineering Structures ;27(2):285_300.
- K. Khy, C. Chintanapakdee, P. Warnitchai, and A. C. Wijeyewickrema, “Modified response spectrum analysis to compute shear force in tall RC shear wall buildings,” Engineering Structures, vol. 180, no., pp. 295-309, 2019.
- K. Leng, C. Chintanapakdee, and T. Hayashikawa, “Seismic shear forces in shear walls of a mediumrise building designed by response spectrum analysis,” Engineering Journal, vol. 18, no. 4, pp. 73-95, 2014.
- L. M. Massone, P. Bonelli, R. Lagos, C. Lüders, J. Moehle, and J. W. Wallace, “Seismic design and construction practices for RC structural wall buildings,” Earthquake Spectra, vol. 28, no. S1, pp. S245- S256, 2012.
- M. Bosc, A. Ghersi, E.M. Marino and P.P. Rossi (2013). “Prediction of the Seismic Response of Steel Frames with Concentric Diagonal Bracings.” The Open Construction and Building Technology Journal, 2013, 7, 118-128.
- Mahmoudi M, Abdi MG. Evaluating response modification factors of TADAS frames. Journal of Constructional Steel Research. 2012 Apr 1; 71:162-70.
- Mander, J.B., Priestley, M.J., and Park, R. "Observed stress-strain behavior of confined concrete." J. Struct. Eng., 114(8), 1827-1849, (1988a).

- Mander, J.B., Priestley, M.J.N., and Park, R. "Theoretical stress-strain model of confined concrete." J. Struct. Eng.,114(8), 1804-1826, (1988b).
- Moehle, J.P., Hooper, J.D., Kelly, D.J., and Meyer, T.R. “Seismic Design of Cast-in-Place Concrete Diaphragms, Chords, and Collectors: A Guide for Practicing Engineers,” NEHRP Seismic Design Technical Brief No. 3, produced by the NEHRP Consultants Joint Venture, a partnership of the Applied Technology Council and the Consortium of Universities for Research in Earthquake Engineering for the National Institute of Standards and Technology, Gaithersburg, MD, NIST GCR 10-917-4, 2010.
- Mondal, A., Ghosh, S., & Reddy, G. R. (2013). Performance-based evaluation of the response reduction factor for ductile RC frames. *Engineering Structures, 56,* 1808–1819.
- Moroder D. Floor Diaphragms in Multi-Story Timber Building. PhD Thesis. Department of Civil Engineering, University of Canterbury, Christchurch, New Zealand; 2016.
- National Building Code of Canada, “Commission on Building and Fire Codes, National Research Council of Canada. Ottawa, Canada, 2010.
- Newmark, N. M., and Hall, W. J. (1982). ‘‘Earthquake spectra and design.’’EERI Monograph Series, Earthquake Engineering Research Institute,Oakland, Calif.
- Pednekar SC, Chore HS, Patil SB. Pushover analysis of reinforced concrete structures. International Journal of Computer Applications. 2015; 975:8887.
- Popovics, S. "A numerical approach to the complete stress-strain curves of concrete." *Cement and Concrete Research,* 3(5), 583-599, (1973).
- Rafael Sabelli PE, Warren Pottebaum SE. Diaphragms for seismic loading. Structural Engineer. 2009 Jan.
- Sadeghi A, Abdollahzadeh G, Rajabnejad H, Naseri SA. Numerical analysis method for evaluating response modification factor for steel structures equipped with friction dampers. Asian Journal of Civil Engineering. 2021 Feb; 22:313-30.
- Schickert, G., and Winkler, H. "Results of tests concerning strength and strain of concrete subjected to multiaxial compressive stresses." *Deutscher Ausschuss fur Stahlbeton,* Heft 277, Berlin, West Germany, (1979).
- Siahpolo, N., Gerami, M., & Vahdani, R. (2016). Inelastic deformation demands of regular steel frames subjected to pulse-like near-fault ground shakings. *International Journal of Advanced Structural Engineering, 8,* 281–296.

- Simo JC, Govindjee S. Nonlinear B-stability and symmetry preserving return mapping algorithms for plasticity and viscoplasticity. Int J Numer Methods Eng 1991;31(1): 151–76.
- Simo JC, Taylor RL. Consistent tangent operators for rate independent elastoplasticity. Comput Methods Appl Mech Eng 1985; 48:101–18.
- Spacone E, Ciampi V, Filippou FC. Mixed formulation of nonlinear beam finite element. Comput Struct 1996;58(1):71–83.
- Sullivan K, Miller TH, Gupta R. Behavior of cross-laminated timber diaphragm connections with self-tapping screws. Engineering structures. 2018 Aug 1; 168:505-24.
- Thorenfeldt, E., Tomaszewicz, A., and Jensen, J.J. "Mechanical properties of high-strength concrete and application in design." *Proc. of the Symposium on Utilization of High-Strength Concrete*, Tapir, Trondheim, Norway, 149-159, (1987).
- Tsai, W.T. "Uniaxial compression stress-strain relation of concrete." *J. Struct. Eng.*, 114(9), 2133-2136, (1988).
- Vassallo D, Christovasilis IP, Follesca M. Design of a four-story Cross Laminated Timber Building in Northern Italy. Wood Design Focus. 2013;23(4):36-44.
- Whittaker A, Hart G, Rojahn C. Seismic response modification factors. Journal of Structural Engineering. 1999 Apr;125(4):438-44.
- William, K.J., and Warnke, E.P. "Constitutive model for the tri-axial behavior of concrete." *Proc., International Association for Bridge and Structural Engineering*, Proceedings, 19, 1-30, (1975).
- Wu, J. P., and Hanson, R. D. (1989).‘‘Inelastic response spectra with high damping’’J. Struct. Div. ASCE, 115(6), 1412–1431.
- Zeynalian, M., Shahrasbi, A. Z., & Riahi, H. T. (2018). Seismic response of cold formed steel frames sheathed by fiber cement boards. *International Journal of Civil Engineering, 16,* 1643–1653.